

NOV 13 1955

Re
tele

to be
Army.

Copy

NBS CIRCULAR 554

Cheyenne Mountain Tropospheric Propagation Experiments

**UNITED STATES DEPARTMENT OF COMMERCE
NATIONAL BUREAU OF STANDARDS**

Related Publications of the National Bureau of Standards

Effective Ground Conductivity Measurements in the United States

Circular 546, 65 cents

- . . . Eighty-four maps are presented in this Circular showing the results of effective ground-conductivity measurements made by various broadcasters and consulting engineers throughout the United States. The need for such detailed maps has long been realized. Over 7,000 radials are shown on the maps, and provisions have been made for entering new measurements, as results become available, for possible future publication.
- . . . Since 1947 the NBS has been cataloging effective ground-conductivity measurements obtained from the files of the Federal Communications Commission. A study of over 7,000 determinations made in the standard a. m. broadcast band was made to see if there was a relationship between effective ground conductivity and surface soil composition.
- . . . The study showed little association of effective ground conductivity with soil type. Previous effective ground-conductivity maps have been prepared on the assumption that the values of effective ground conductivity are fairly highly associated with soil types; the use of such maps has shown them to be inaccurate in many cases. The present publication was designed to help correct this situation.

Radio-Frequency Power Measurements

Circular 536, 15 cents

- . . . Controlled utilization of radio-frequency power necessitates accurate methods of measurement. Although originally used solely in communications, radio-frequency power is now being widely applied in many fields, especially in medicine and industry, whenever heating, not dependent on the normal methods of heat transfer, is required. Also new and extensive applications are being found for radio-frequency power in navigational devices and scientific research. This increasing use makes clear the necessity for accurate methods of measurement. Many technical considerations accentuate the difficulty of making accurate measurements, and every application of radio-frequency power requires separate investigation for determination of the most practical measurement method.
- . . . This Circular presents a comprehensive survey of the methods currently in use and gives a brief discussion of the theoretical background, practical limitations, and advantages of these methods. The Circular contains sections on calorimetry, substitution methods, single-variable devices, two-variable devices, and directional couplers. It is well illustrated with 27 figures. A comparative table and a list of references are appended.

Cheyenne Mountain Tropospheric Propagation Experiments

A. P. Barsis, J. W. Herbstreit,
and K. O. Hornberg



National Bureau of Standards Circular 554

Issued January 3, 1955

Contents

	Page
1. Introduction.....	1
2. System selection.....	1
2.1. Transmitting and receiving sites.....	1
2.2. Transmitting equipment.....	2
2.3. Receiving and recording equipment.....	2
2.4. Meteorological equipment.....	2
3. Description of facilities.....	2
3.1. Transmission paths.....	2
3.2. Transmitting facilities.....	5
a. General.....	5
b. Ultra-high frequency transmitter—1,046 Mc.....	6
c. Very-high frequency transmitters—92, 100, 192.8, and 210.4 Mc.....	9
3.3. Recording facilities.....	10
a. Ultra-high frequency receivers—1,046 Mc.....	10
b. Very-high frequency receivers—92, 100, 192.8, and 210.4 Mc.....	13
c. Special receiving equipment.....	13
d. Recording devices.....	15
3.4. Meteorological facilities.....	15
4. Operations.....	17
4.1. Transmitter operations.....	17
4.2. Receiver servicing and calibration.....	17
4.3. Meteorological observations.....	18
5. Data analysis.....	19
5.1. General.....	19
5.2. Recording charts.....	20
5.3. Time totalizer data.....	24
5.4. Study of long-term variations.....	24
5.5. Study of short-term variations.....	26
5.6. Study of prolonged space-wave fadeouts on 1,046 Mc.....	26
5.7. Other studies.....	29
5.8. Analysis of meteorological observations.....	29
6. Preliminary results in terms of theory.....	31
6.1. General.....	31
6.2. Propagation within the radio horizon.....	31
6.3. Propagation in the diffraction region.....	32
6.4. Propagation far beyond the radio horizon.....	33
7. References.....	38
8. Appendix. Calculation of the angular distance, θ , over irregular ter- rain.....	39

Cheyenne Mountain Tropospheric Propagation Experiments

A. P. Barsis, J. W. Herbstreit, and K. O. Hornberg

The National Bureau of Standards has established extensive facilities for studies of tropospheric radio-wave propagation in the very-high frequency and ultra-high frequency portion of the frequency spectrum at Cheyenne Mountain, Colorado. These facilities include high-power continuous-wave transmitters on five frequencies, from 92 to 1,046 Mc. Continuously recording field-strength receivers are located at four fixed receiving locations ranging to 226 miles from Cheyenne Mountain, with provisions for semifixed recordings at Anthony, Kans., and Fayetteville, Ark., which are 393 and 617 miles, respectively, from the transmitter site. An extensive radio meteorological installation is located at Haswell, Colo., where accurate measurements of temperature, pressure, and humidity are made with electronic measuring devices, and refractive-index turbulence is measured with the microwave refractometer developed at the Bureau. These facilities are described and sample results are reported. The new theory of tropospheric propagation embodying the Booker-Gordon scattering principles as extended by Staras is related to the measurements.

1. Introduction

The Central Radio Propagation Laboratory of the National Bureau of Standards established the Cheyenne Mountain Field Station at Colorado Springs, Colo. in June 1950 in order to determine tropospheric propagation characteristics within, near, and far beyond the radio horizon for the 50-Mc to 30,000-Mc frequency band. Acceleration of certain phases of the program was supported in part by the Air Navigation Development Board and the U. S. Army Signal Corps.

The basic experimental program of investigation includes special studies of the effects of rough terrain and correlation with meteorological data. Transmissions have been made continuously on representative frequencies in the neighborhood of 100, 200, and 1,000 Mc from antenna installations at various heights above the surrounding terrain. Recordings of radio-transmission loss have been

made simultaneously at four fixed and two semifixed locations at various distances from these signal sources, and meteorological conditions have been investigated and recorded at one point along these transmission paths. Fundamental theoretical studies of the variables frequency, antenna height, distance, terrain, and meteorological characteristics have been undertaken concurrently in order to provide a means of extrapolating the results obtained from the study to a wide variety of systems involving radio propagation in this range of frequencies. These studies include effects of rough terrain, dependence of transmission loss on refractive-index profiles, height-gain functions, and the application of scattering and related theories to the interpretation of long- and short-term field variations.

2. System Selection

2.1. Transmitting and Receiving Sites

In order to obtain transmission paths simulating air-to-ground communications, transmitting sites at the east slope of the Front Range of the Rocky Mountains near Colorado Springs, Colo., were selected, and transmissions beamed to receiving sites located on the plains of eastern Colorado and Kansas. The sheer face of Cheyenne Mountain provided the location most closely approaching an airborne transmitter, and two sites for permanent operation were selected; one about half-way up and one near the summit of the mountain. Both sites are accessible by an all-weather road. In addition thereto, a rhombic antenna installa-

tion is available at Camp Carson, near the base of Cheyenne Mountain, and provisions are made for installation of a Yagi type, or similar medium-gain antenna, on the summit of Pikes Peak for operation during the summer months, when the summit is accessible. The latter two sites have been used intermittently.

Receiving sites were selected along a radial of about 105 degrees east of true north from the transmitter sites in order to permit similar orientation of all transmitting antennas to produce maximum usable power at all receiving sites. The 105-degree direction roughly intersects the Arkansas River valley in eastern Colorado and western Kansas.

2.2. Transmitting Equipment

Inasmuch as one of the primary objectives of the program consisted in the study of fields far beyond the radio horizon, maximum continuous wave-power output from highly stable (in frequency and output) transmitting apparatus had to be obtained. For the 100- to 200-Mc range commercial equipment was available, which required little modification, and provides an average power output up to 3 kw. As no commercial transmitters were available for the 1,000-Mc range, a development program was initiated toward procurement of a klystron-type high-power transmitter capable of operating in the 1,000-Mc range. At each of the two permanent transmitter sites on Cheyenne Mountain, two VHF transmitters were installed, one in the 100-Mc and one in the 200-Mc range. Due to the cost of the 1,000-Mc equipment only one UHF transmitter was built, and installed at the Cheyenne Mountain summit site. In addition, a 1-kw commercial FM transmitter was installed in a truck for semimobile operation. All transmitters, including the UHF installation, are capable of being modulated by tone or voice.

In order to provide a sufficient amount of effective radiated power and to prevent reflections from the mountain slopes, a specially designed horn-type radiator was installed at the summit site for use with the 1,000-Mc transmissions. For the VHF transmissions corner-reflector-type antenna systems are used on Cheyenne Mountain.

For optimum system performance the frequencies of the transmitters have to be maintained so that the emissions will remain within the acceptance band of the receivers. Direct crystal control, as well as control through suitable multipliers from a common secondary frequency standard, is used, together with appropriate monitoring facilities. Constant power is maintained by monitors in the output circuits of the VHF transmitters, calibrated water loads being used as the standards.

2.3. Receiving and Recording Equipment

To obtain adequate reception of transmissions in both the VHF and UHF bands at distances far beyond the radio horizon, receivers having excellent sensitivity were considered necessary. Such receivers inherently require narrow band-

width and low noise figure. Considerations of the state of the art, financial aspects, and desired delivery date led to the choice of establishing a desired bandwidth of approximately 500 cycles, with a noise figure of 6 to 10 db. In order to maintain frequency stability in conformance with the transmitters, a secondary frequency standard is utilized, from which local oscillator frequencies are derived. Calibration of the receiving equipment is provided by suitable signal generators, which are checked periodically against laboratory standards.

Recording devices that will operate continuously without constant supervision are required. Recording milliammeters are consequently provided at all receiving sites. These are driven directly from specially designed receiver output circuits. In order to facilitate and improve the accuracy of the analysis of records of rapid signal variations, time-totalizing equipment, also operated from receiver-output circuits, is employed where necessary. The time totalizers drive counting motors coupled to indicator dials, which are automatically photographed at regular intervals by relay-operated cameras. Thus, microfilm records of the total times that the signal exceeds several predetermined levels are available for evaluation in addition to the graphical records.

2.4. Meteorological Equipment

It was considered essential that meteorological information should be available over the transmission path simultaneously with the results of the radio-wave propagation experiment. Experiments disclosed that the frequent high winds in eastern Colorado precluded the extensive use of wire-sonde, or similar equipment, and dictate the use of fixed recording instruments. A 500-ft tower at the receiving site just beyond the radio horizon allows installation of all types of meteorological recording equipment, including equipment for measuring the gradient of the refractive index directly at various heights above the ground up to the 500-ft maximum height. At other points along the transmission path, records of temperature, humidity, and pressure are obtained at the surface by conventional recording devices. This is considered to be a minimum meteorological installation and will undoubtedly have to be expanded as further experience is obtained.

3. Description of Facilities

3.1. Transmission Paths

The Cheyenne Mountain transmission paths are shown pictorially in figure 1 with the fixed transmitter sites on Cheyenne Mountain and the sites for the semimobile transmitter at the base of the mountain near Camp Carson and on top of Pikes Peak.

Cheyenne Mountain rises abruptly from a

plain, which has an elevation approximately 6,000 ft above sea level. The Camp Carson site is on the plain at 6,220 ft, and the Pikes Peak site is at 14,100-ft elevation.

Several fixed and semimobile recording sites are located in eastern Colorado, Kansas, and Arkansas. Figures 2, 3, and 4 show the terrain profiles along the transmission paths from the summit transmitter to each of the three fixed recording

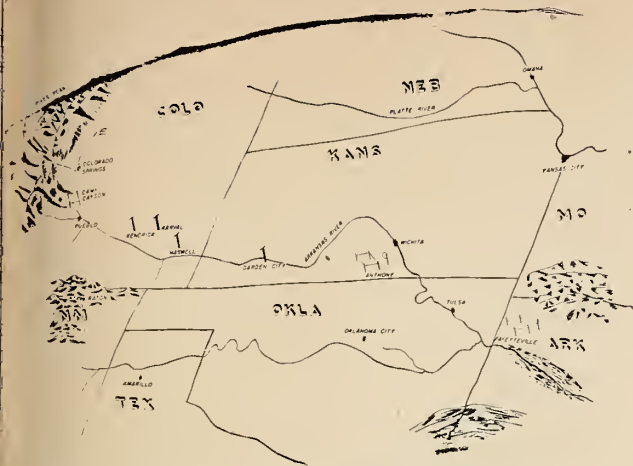


FIGURE 1. Pictorial view of Cheyenne Mountain transmission paths.

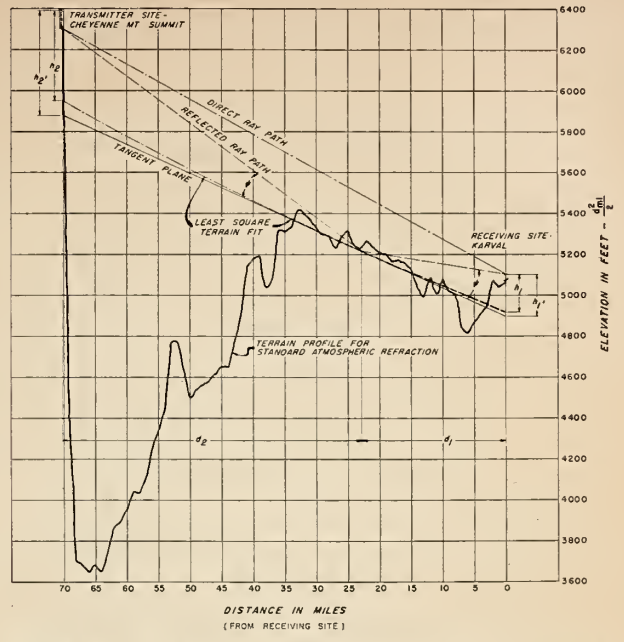


FIGURE 3. Geometry for space-wave calculations for path between summit transmitter site and Karval receiving site. Ray paths shown are for 1,046-Mc transmissions.

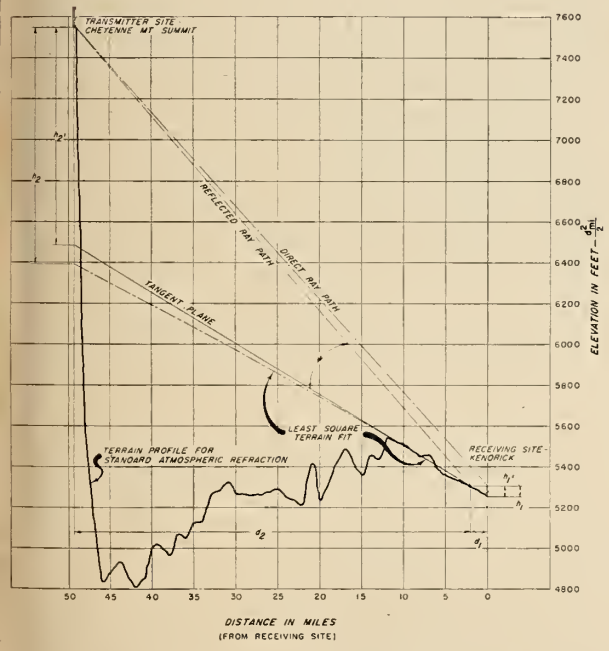


FIGURE 2. Geometry for space-wave calculations for path between summit transmitter site and Kendrick receiving site. Ray paths shown are for 1,046-Mc transmissions.

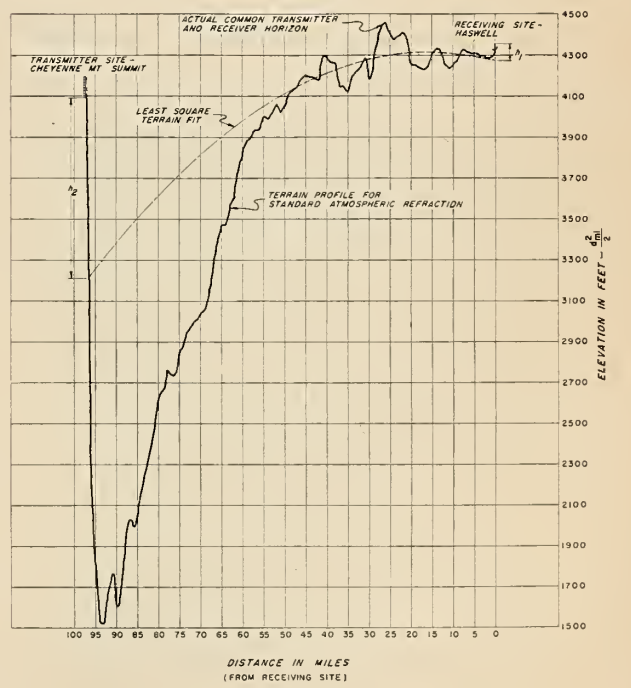


FIGURE 4. Geometry for diffraction calculations for path between summit transmitter site and Haswell receiving site.

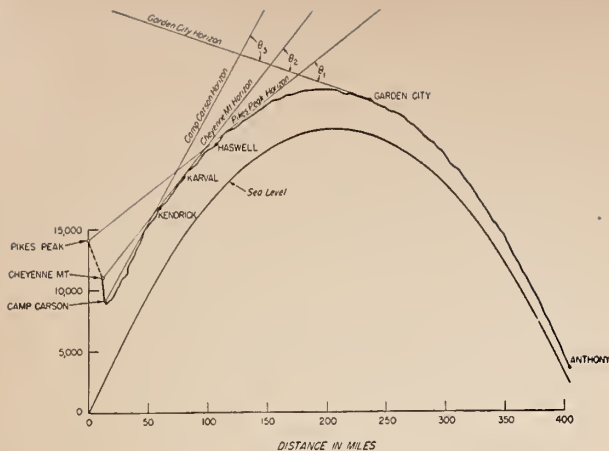


FIGURE 5. Terrain profile of Colorado-Kansas paths.

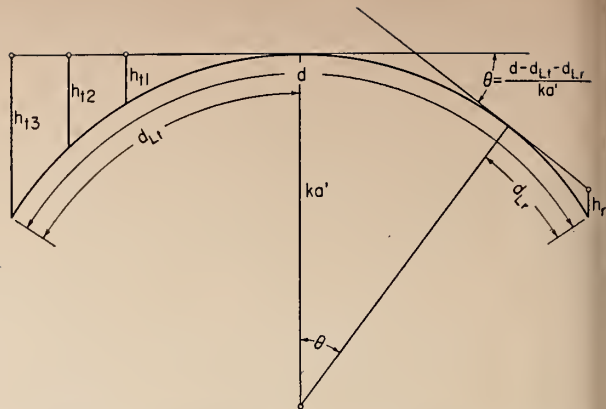


FIGURE 6. Parameter θ in tropospheric wave propagation.

sites located at Kendrick (49.3 mi), Karval (70.2 mi), and Haswell, Colo., (96.6 mi). Figure 5 shows the terrain profile out to Garden City and Anthony, Kans. The definition is given on figure 5 of an angle θ , which has been used throughout this report to characterize a particular transmission path. This is the angle between lines shown in the great circle plane from the transmitting and receiving antennas to their respective horizons. Transmission paths within the radio horizon will be characterized by negative values of θ , and positive values of θ correspond to paths extending beyond the radio horizon. The usefulness of the parameter θ in tropospheric propagation lies in the fact that it can be used to describe fading characteristics and values of transmission loss, and at the same time it can be used to extrapolate the results of propagation measurements to a terminal at an arbitrarily high elevation. Figure 6 demonstrates how the angle θ can characterize various transmitting heights h_{11} , h_{12} , and h_{13} . This principle is of great importance in engineering air-to-ground communication and navigation systems. The method of calculating θ for transmission paths over irregular terrain is discussed in the Appendix, and the values of θ for all Cheyenne Mountain transmission paths are given in table 4, based on an assumed gradient of refractive index equal to -39.23 N-units per kilometer to allow for standard air refraction. The terrain profiles of figures 2, 3, 4, and 5 allow for standard atmospheric refraction in order to make the radio rays appear as straight lines and show that the Kendrick and Karval sites are within the radio horizon of the Cheyenne Mountain summit site, while the Haswell site is just beyond the radio horizon in the diffraction region. The Garden City location is well beyond the radio horizon and considered out of the diffraction region and in the scattering region for reception. An examination of these

terrain profiles in the light of Rayleigh's criterion of roughness indicates that the actual terrain is quite rough compared to the wavelength of transmissions (especially on 1,046 Mc), although the transmission path appears visually to be as level as one is likely to find in siting VHF or UHF ground terminals. The practical significance of this roughness is discussed in some detail in a later section of this paper.

Tables 1 and 2 show pertinent data for all transmitting and receiving sites. The soil along the transmission paths in eastern Colorado and western Kansas is very arid; it is utilized principally for cattle grazing and dry farming. Further east, in the vicinity of Garden City and extending to Anthony, the land is less arid and wheat farming predominates.

The prevailing winds, as measured by recording wind-direction equipment, are usually from the south, with turbulence expected at all levels extending from the mountain region to the Colorado-Kansas border. Wind velocities in the Colorado Springs and Haswell, Colo. areas are

TABLE 1. Transmitting locations

Location	Frequency	Latitude	Longitude	Antenna	
				Elevation above mean sea level	Maximum gain relative to an isotropic radiator
Cheyenne Mt. sum- mit.....	100	38.764	104.864	8,805	10.0
	192.8			8,855	10.4
	230			8,855	10.8 ^a
Cheyenne Mt. base.....	1,046	38.774	104.862	8,760	26.0
	92			7,485	9.3
	210.4			7,505	10.6
Camp Carson.....	236	38.696	104.830	7,505	10.9 ^a
Pikes Peak.....	100	38.839	105.042	6,260	19.5
	100			14,115	8.6

^a Estimated.

a. General

Transmitting facilities at the Cheyenne Mountain fixed sites include four commercial FM transmitters for the VHF range, and one CW-UHF transmitter with a klystron output tube rated at 4-kw average power. The Cheyenne Mountain summit site houses the UHF transmitter, operating on a frequency of 1046.4748 Mc; one 3-kw commercial transmitter operated on 100 Mc; and one somewhat modified commercial transmitter operated on 192.8 Mc. These transmitters were originally designed for frequency modulation broadcasting but are not modulated in these operations. The lower site on Cheyenne Mountain (usually referred to as the "base site") houses similar VHF transmitters operated on 92 Mc and 210.4 Mc, respectively. Due to the increase of commercial VHF television facilities in the area since the fall of 1952, the transmitters in the 200-Mc range are being modified to operate at 230 Mc (at the summit site) and 236 Mc (at the base site.) The new frequencies will permit full utilization of the facilities without interfering with commercial television operations.

Figure 7 shows the summit site facilities, and illustrates the abrupt slope of Cheyenne Mountain.



FIGURE 7. Cheyenne Mountain summit site.

RECEIVING LOCATIONS

Site-No.	Location	Latitude	Longitude	Elevation of the local ground above mean sea level
1.....	Kendrick.....	<i>deg</i> 38. 569	<i>deg</i> 103 984	<i>ft</i> 5, 260
2.....	Karval.....	38. 632	103. 572	5, 060
3.....	Haswell.....	38. 383	103. 141	4, 315
4.....	Garden City ^a	37. 833	100. 858	2, 855
5.....	Anthony.....	37. 240	97. 898	1, 335
6.....	Fayetteville.....	36. 107	94. 107	1, 325

ANTENNAS AT SITES 1 TO 4 (all dipoles)

Frequency	Elevation above ground level
<i>Mc</i>	<i>ft</i>
92	36. 75
100	18. 75
192. 8	17. 5
210. 4	35. 5
230	17. 5
236	35. 5
1, 046	42. 67

ANTENNAS AT SITE 5

Antenna	Frequency	Elevation above ground level	Maximum gain relative to isotropic radiator
	<i>Mc</i>	<i>ft</i>	<i>db</i>
Rhombic A.....	100	39	18. 6
Rhombic B.....	92	39	12. 85
Rhombic B.....	192. 8	39	12. 0
Rhombic B.....	210. 4	39	14. 45
Yagi.....	100	39	12. 05
Parabolic reflector.....	1, 046	8. 5	25. 65

ANTENNAS AT SITE 6

Antenna	Frequency	Elevation above ground level	Maximum gain relative to isotropic radiator
	<i>Mc</i>	<i>ft</i>	<i>db</i>
Rhombic.....	92	38	15. 0 ^b
Rhombic.....	100	38	19. 95
Parabolic reflector.....	1, 046	38	26

^a A parabolic reflector was used at certain times for 1,046-Mc operation, having a gain of 25.65 db relative to an isotropic radiator and located 8.5 ft above ground.

^b Estimated.

generally in excess of 15 mph with gusts frequently exceeding 50 mph. The area is one of conflict between the settled conditions of mountain induced subsidence and solar induced turbulence. The area is under intensive study by meteorologists as the birthplace of tornadoes, and the Geophysical Research Directorate is conducting an intensive turbulence study in this area. Although the locale for these propagation measurements was chosen primarily because of the availability of a high mountain site, subsequent investigation has revealed the area to be an excellent location for radio-meteorological studies due to the heterogeneous conditions available.

b. Ultra-High Frequency Transmitter—1,046 Mc

The 1,046-Mc transmitter was specially built for the National Bureau of Standards. Its installation in the summit building on Cheyenne Mountain is shown in figure 8. It was designed to meet the rigid specifications of the narrow-band, continuous-wave radio-propagation system for Cheyenne Mountain, but also has provisions for modulation. This transmitter meets the essential system requirements of radiating a high-power, essentially monochromatic, stable, continuously monitored radio-frequency signal at 1,046.4748 Mc. It is described in more detail than the VHF units because the transmitter is unique in having the highest continuous power output of any 1,000-Mc transmitter in the country. The transmission system consists of four major components. They are (1) the crystal driver unit, (2) the klystron power amplifier, (3) the direct-current power supplies, and (4) the antenna systems. A block diagram of this transmitter is shown in figure 9.

(1) *The crystal driver unit.* The basic requirements for a driver unit for this type of transmitter are very exacting and necessitate the employment of a number of rather unusual design features. The first of these requirements is that an extremely stable basic crystal source be used so that multiplication of the output frequency of the crystal standard 10,368 times could result in an essentially monochromatic output with a long-term variation of less than 250 cycles at 1,046 Mc. A secondary frequency standard was selected to meet these requirements. For reasons of technical simplicity in the receivers, the output frequency desired is not an exact multiple of 100 kc. A crystal unit approximately 1 percent higher was used. The manufacturer cooperated with the Central Radio Propagation Laboratory in this problem by designing this special crystal at 100.93315 kc and performed appropriate tests to verify adequate performance. Experience has shown that the actual total variation between two standards is less than 125 cycles at the final 1,046-Mc frequency over a 6-month period.

The second requirement is that the driver output at 1,046 Mc should be free of all types of modulation and noise, and have a constant power output. To accomplish these results, considerable effort was spent in the design of this unit. The plates and filaments of all tubes are operated on well-filtered, d-c regulated supplies, which are in turn supplied through a-c regulators. To reduce spurious outputs and unwanted modulation components, the stages are arranged as follows: All of the low- and medium-frequency multiplier stages consist of two tubes with the grids connected in push-pull and plates connected in parallel for the doublers, or both grids and plates, in push-pull for the triplers. All of the input and output circuits have high Q , are double tuned and slightly under-coupled. The radio frequency drive on all stages

is sufficiently high so that the transconductance of tube can drop to 50 percent of its normal value without affecting the over-all output of the transmitter. In practice it has been possible to operate at full output for a period of several weeks with the tubes in two of the stages having transconductances of less than 20 percent of normal values. The single tube high-frequency multiplier stages are grounded-grid, coaxial-cavity type multipliers. In these stages, as in the lower frequency strip, all of the above described precautionary measures against unwanted modulation components are employed.

(2) *The klystron power amplifier.* The final amplifier consists of a 4 kw output, three-cavity, klystron tube and associated components. This type of tube in itself presents a unique solution to the high power problem in this frequency range. The tube is a low-efficiency device, generally of the order of 20 to 25 percent, but this disadvantage is greatly offset by the extremely high gain of the tube in this circuit (400). The arrangement of the tube elements is shown in figure 10. Basically, the tube operates as follows: The filament is heated from a 6-v d-c supply and requires a current of approximately 50 amp for normal operation. The difference in potential between the cathode and filament is 2,200 v, which produces by electron bombardment the heating of the tantalum cathode, the primary source of the electron beam. A further difference in potential of 11,000 v exists between the cathode and the body of the tube, which in turn produces the high-velocity electron stream moving through the drift space and the cavities. These electrons are absorbed by the catcher or bucket which is thereby heated. This heat is removed by a large-capacity water-cooling system. The operation of the tube is similar to that of low-powered klystron tube types, except that the electron beam is magnetically confined to the correct path by use of three focusing coils around the cavities.

A more detailed discussion of klystron operation and performance may be found in articles by Varian [1]¹ and by Hiestand [2].

A number of rather interesting circuits have been employed to maintain constant power output from the tube under operating conditions. For example, since the electron emitter source is operated as a temperature-limited device, it is necessary to maintain the input power to the filament-cathode constant. This is accomplished in the following manner: The cathode supply is regulated to keep the cathode temperature as nearly constant as possible in order to maintain the temperature-limited beam current at a constant value. This circuit uses a saturable core reactor which has one primary and two secondary windings. The primary is in series with the transformer which supplies the klystron with its filament power. The basic function of the reactor is

¹Figures in brackets indicate the literature references at the end of this paper.

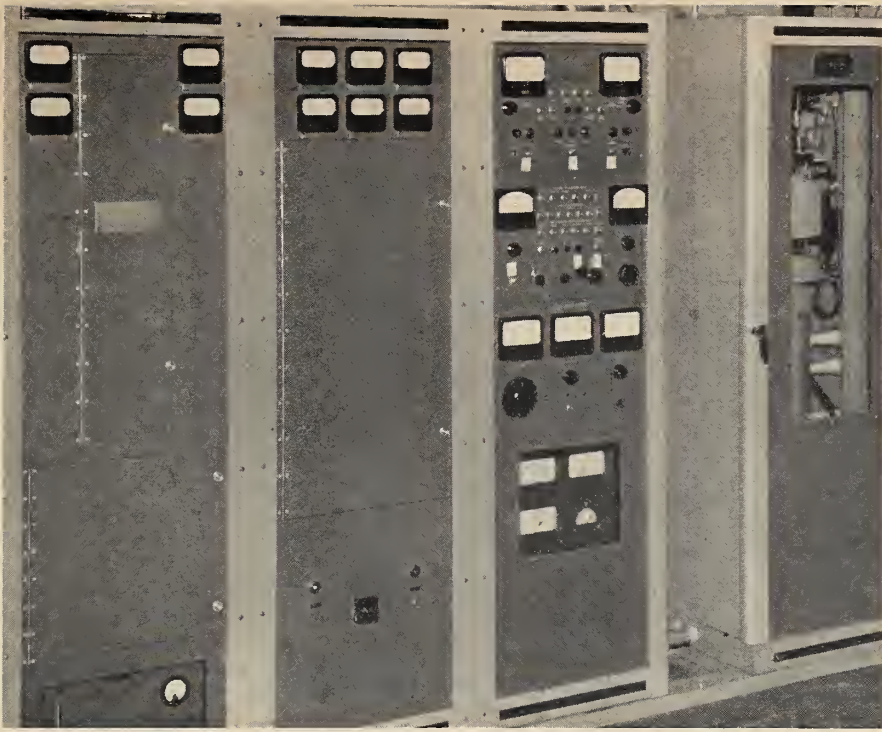


FIGURE 8. 1,046-Mc transmitter.

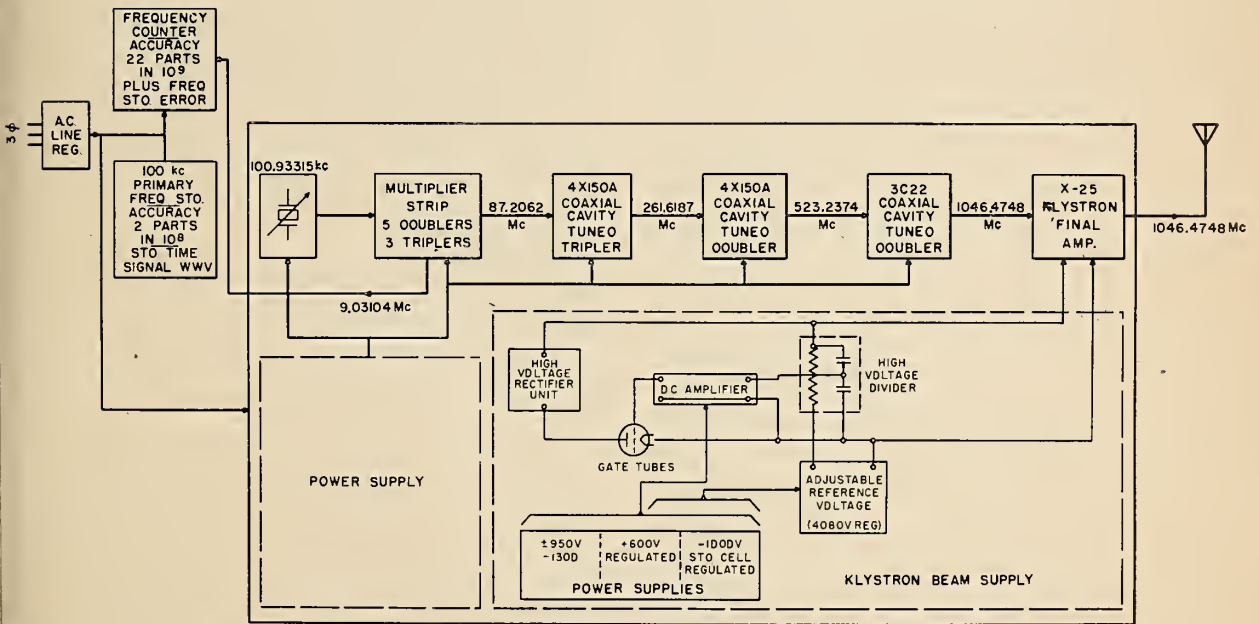


FIGURE 9. Block diagram of 5-kw, 1,046-Mc transmitter.

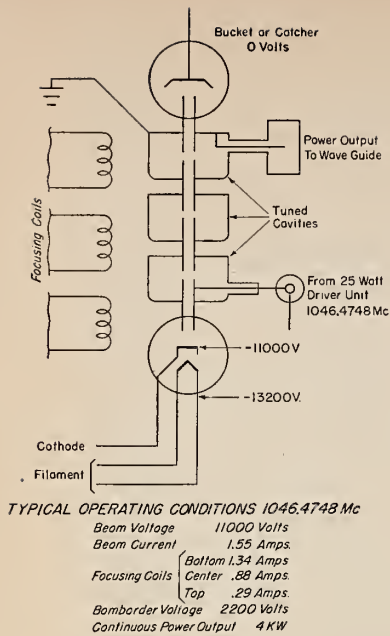


FIGURE 10. Arrangement of elements in 1,046-Mc klystron tube.

to control the impedance of this primary winding and thus control the filament power. The filament is operated temperature-limited so that a decrease in reactor primary impedance will increase the filament power and so increase the cathode current and temperature. One of the secondary windings is a bias coil. The bias current is made up of a constant current plus a compensating current which decreases when the line voltage increases. The constant current is about four times that of the compensating current and sets the level of saturation of the reactor and therefore the level of the filament power. The second of the reactor secondary coils carries the cathode current. The current in this coil has an effect opposite to the current in the bias coil. The reactor is designed so that an increase in the cathode current will increase the impedance of the reactor coil primary and so decrease the filament power. This prevents the cathode current from becoming excessive due to back heating effects. The saturable reactor prevents this running away because an increase in cathode current causes a decrease in the filament power to compensate for the increase in back heating. However, this effect is not large enough to keep the cathode power constant with changes in line voltage. If only the cathode coil of the reactor were sensitive to changes in line voltage, an increase in line voltage would cause an increase in cathode voltage and a small increase in current would result. Therefore, the bias current is also made sensitive to line voltage in such a way that an increase in

line voltage causes a decrease in cathode current sufficient to keep the cathode power almost constant. This is accomplished by making the compensating portion of the bias current decrease with an increase in line voltage. This in turn reduces the total bias current and therefore the filament power and the cathode power, thus giving the overall effect.

Approximately 12 kw are dissipated in the form of heat in the klystron bucket under normal operating conditions. Cooling water is circulated through the klystron catcher bucket and the tube body, using a pump for circulation and an external radiator for cooling. The water for the catcher bucket is metered with a flowmeter and a thermometer. These are both connected electrically into the beam voltage supply, so that a failure of water flow or excessive temperature will automatically remove the beam voltage. The body water flow is determined by two pressure gauges with associated interlock circuits so that a failure of body water flow will turn off the klystron filament, cathode, and beam voltages.

The last major unit of the klystron power circuits is the regulated focus coil supply. This supply furnishes current for the three focus coils. The current in the top and center coils flows in the same direction but the current in the bottom coil flows in the opposite direction. The purpose of the bottom coil is to counteract the effects of the two top coils on the formation of the electron beam at the cathode.

Some of the electrons in the beam are attracted to the cavity structure resulting in a small "body" current. This current is dependent primarily upon the focus coil currents, but is also influenced by the degree of RF modulation or bunching in the electron beam. The power gain and output of the klystron are also a function of the focus conditions of the beam. In practical operation, currents in the focus coils are adjusted to give maximum output power while keeping the body current minimized.

(3) *The beam power supply.* The power supply consists of three basic units: (1) the high voltage rectifier unit and associated a-c control circuits, (2) the d-c regulator unit, and (3) the control panel. The power unit operates on three-phase 208 to 230 v a-c and is capable of supplying 14,000 v d-c at about 2.0 amp.

The operation of the power supply as a unit can best be described in conjunction with the description of the regulator unit. The regulator unit consists of a two-stage d-c amplifier, an adjustable reference voltage source, regulated power supplies, and the high-voltage divider. The operation is such that the high-voltage divider balances the high negative output voltage against the positive reference voltage. The voltage unbalance signal from the divider is fed to the d-c amplifier and after amplification appears as a large controlling voltage at the grids of the gate tubes. This voltage on the grids of the gate tubes alters their

conduction in such a direction as to minimize the unbalance signal at the input of the d-c amplifier. Thus, within the limits of the amplifier and the gate-tube range, the output voltage is quite closely proportional to the reference voltage. LC filters are not used, the filtering and regulation being entirely dependent upon electronic circuits. The basis for this exact regulation is the use of five standard cells as a reference voltage source. In this way the two standard reference supplies (for the d-c amplifier and tubes in the high-voltage reference supply) are maintained within a few millivolts of rated voltage. As an example, the high-voltage reference supply will show a change of less than 5 v at 4,850 v with the input line voltage changing from 212 to 248 v.

The high-voltage rectifier unit consists of two full wave 3-phase systems connected in series, and arranged to produce the equivalent of a 12-phase system. The gate tubes consist of four type 3X2500F3 tubes in parallel. The entire rectifier system can be controlled remotely from the transmitter control panel, thus greatly simplifying transmitter operation.

(4) *The antenna and power measuring system.* The antenna system consists of two moderate gain antennas and associated feed systems. The first, for horizontal polarization only, is a slot-fed, tapered array, guided by a divided horn. With this arrangement side lobes are attenuated to below the 20 db level while the vertical beam width is maintained at 6 degrees, and the horizontal at 18 degrees. The second system is a parabolic section illuminated by a horn, with the horn feed so arranged that either horizontal or vertical polarization can be used. The patterns and side-lobe conditions are essentially the same in each polarization as for the first antenna. Both antennas are tuned at the feed points by double stub tuners, thus maintaining a low standing-wave ratio in the $3\frac{1}{8}$ in. coaxial line and allowing maximum power transfer from the transmitter.

The transmitter output power is measured by a wattmeter which is essentially a coaxial water load with provision made for measuring the temperature rise of the water flowing through the load. The calorimetric load is made from standard $3\frac{1}{8}$ in. line by a gradual transition from air-to-water around the center conductor. The radio-frequency power is absorbed in the water as it flows through the load. The input and output water temperature are measured and the power calculated therefrom.

In addition, a continuous monitor is provided in the form of a Bethe-hole directional coupler, crystal detector, tuning stub, and power meter. This meter reads the forward power flowing from the klystron towards the load. When the load is well matched the meter indicates the power out-

put of the transmitter directly. It is calibrated against the water load at regular intervals.

c. Very-High Frequency Transmitters—92, 100, 192.8, and 210.4 Mc

The 92-Mc transmitter installed on Cheyenne Mountain at the base site and the 100-Mc transmitter installed at the summit site are conventional commercial 3-kw FM-broadcast transmitters with provision for the use of a high-stability crystal controlled frequency source and primary voltage regulation. They have been operated at 2-kw output.

The 192.8-Mc transmitter at the summit site and the 210.4-Mc transmitter at the base site are adaptations of conventional commercial FM transmitter driver circuits with the addition of a final power amplifier and doubler. These are interesting in that conventional type 3X2500A3 triodes, although not normally employed at such high frequencies, were used for economic reasons and to simplify construction. These have given consistently reliable performance with a tube-life averaging well over 4,000 hours producing a continuous output power of 2 kw. The frequency control of these transmitters also has provisions for more stable crystal control. Figure 11 shows a block diagram of the VHF transmitters.

Modification of the two 200-Mc transmitters to the still higher frequencies is in progress, but it is expected that 2-kw output power will not be obtained at 230- and 236-Mc operation without replacing the 3X2500A3 tubes in the final amplifier with tubes designed for operation at these higher frequencies.

The antennas for all frequencies from 92 to 236 Mc are horizontally polarized corner reflector types driven by half-wave dipoles and matched to 50-ohm $3\frac{1}{8}$ in. coaxial transmission lines. These antennas have gains of approximately 10 db relative to an isotropic radiator and directivity patterns such that only a small amount of the radiated energy strikes the mountain behind and below them. Figure 7 illustrates the position on the tower of two of the corner reflector antennas at the summit site. The power output of the transmitters is continuously monitored with an indicator periodically calibrated against a commercial wattmeter.

In addition to the VHF transmitters described above, a 1-kw commercial type FM transmitter operating on 100 Mc has been installed in a van-type truck. This semimobile transmitting system has been used at the Camp Carson and Pikes Peak sites. The power output, voltage regulating, and frequency-control systems of this transmitter are essentially the same as described for the fixed installations. The frequency of 100 Mc was chosen in order to take advantage of existing receivers, but it is feasible to operate the transmitter at other frequencies between 92 and 108 Mc.

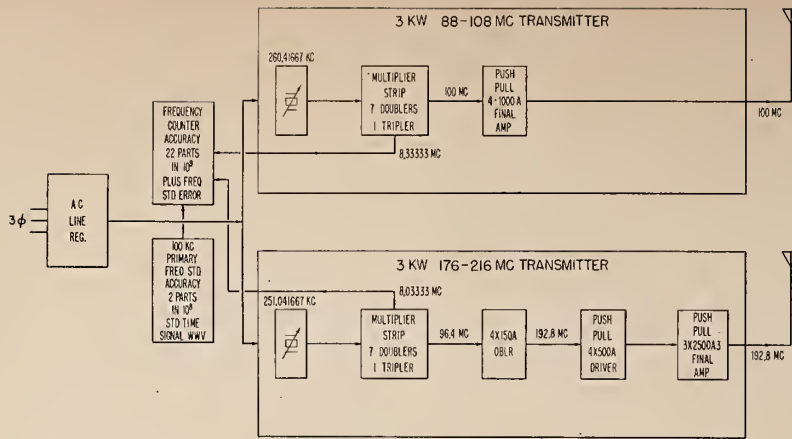


FIGURE 11. Block diagram of 88- to 108-Mc and 178- to 216-Mc transmitters.

Operation on 100 and 192.8 Mc.

3.3. Recording Facilities

Recording locations were established in eastern Colorado, Kansas, and Arkansas and instrumentation effected to permit continuous unattended operation. Pertinent information regarding the sites, their locations, distances from the transmitter, as well as values for the angle θ (see above) is shown in tables 2, 3, and 4. The Kendrick,

Karval, Haswell, and Garden City sites are permanent and record all five frequencies continuously. The Anthony and Fayetteville sites are semipermanent and record for desired periods during the summer and winter on two or more frequencies.

The permanent sites utilize dipole receiving antennas while the more distant sites use rhombic or parabolic reflector type antennas to obtain higher gain. Figures 12 and 13 are photographs of typical fixed and semimobile recording sites. Figure 14 is a block diagram of a typical fixed recording site.

TABLE 3. Distances in miles

Receiver	Transmitter			
	Cheyenne Mountain		Camp Carson	Pikes Peak
	Summit	Base		
Kendrick.....	49.3	49.4	46.6	60.0
Karval.....	70.2	70.2	68.0	80.5
Haswell.....	96.6	96.8	93.8	107.4
Garden City.....	226.5	226.6	223.6	237.1
Anthony.....	393.5	393.6	390.7	404.1
Fayetteville.....	617.7	617.7	614.0	628.1

a. Ultra-High Frequency Receivers—1,046 Mc

The 1,046-Mc receiver was designed and constructed with major considerations for narrow-band characteristics, extreme frequency stability, and high-gain stability. The receiver has a signal bandwidth of approximately 500 cycles between points 1 db down from the maximum response. A noise figure of approximately 11 db has been attained in this receiver. This narrow bandwidth

TABLE 4. Angle θ in milliradians

For standard atmosphere ($\Delta N = -39.23/\text{km}$)

Receiver	Transmitting antenna and frequency						
	Cheyenne Mountain					Camp Carson	Pikes Peak
	Summit		Base				
	100 Mc	192.8 Mc (230)	1,046 Mc	92 Mc	210.4 Mc (236)	100 Mc	100 Mc
Kendrick.....	-3.18	-3.29	-3.72	+1.01	+0.95	+5.64	-10.27
Karval.....	-1.33	-1.45	-1.35	+4.11	+4.02	+8.53	-9.12
Haswell.....	+1.81	+1.68	+1.75	+6.48	+6.39	+11.54	-5.36
Garden City.....	+28.1	+28.1	+26.7	+31.3	+31.3	+38.4	+20.6
Anthony.....	+58.5	+58.4	+59.8	+63.5	+63.4	+68.0	+50.9
Fayetteville.....	+98.3	+98.2	+105.0	+103.2	+103.1	+107.8	+90.6

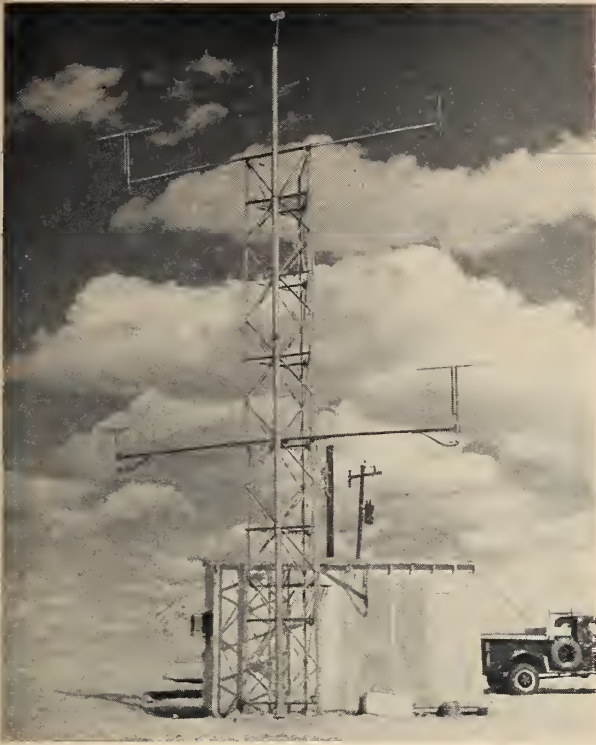


FIGURE 12. *Typical fixed recording site.*



FIGURE 13. *Typical mobile recording site.*

and low noise figure yield a sensitivity, P_{ms} , of approximately 160 db below 1 w ($0.07 \mu\text{v}$ across the 50-ohm receiver terminals). Figure 15 is a block diagram of this 1,046-Mc narrow band receiver. The receiver is of the double superheterodyne type with the local oscillators crystal-controlled from multiplier chains operating from a 100-ke primary frequency standard. The output circuits of this receiver were designed specifically to operate with 1-5 ma strip-chart recorders and 0 to 10 v high-impedance totalizing equipment. This receiver has both linear and logarithmic responses with the logarithmic response having dynamic ranges of 0 to 20 db, 0 to 40 db, and 0 to 60 db. The receiver consists of a number of integral units which may be removed separately. The first of these major units is a preselector of the coaxial cavity type. The selectivity of this tunable coaxial cavity is such that signals 25 Mc either side of resonance are attenuated by 30 db. This unit has an insertion loss of approximately 1 db at the 1,046 Mc operating frequency. The signal out of the preselector is fed to the next component of the system, which is a coaxially-mounted crystal mixer of conventional design. The third component of the receiver is a crystal multiplier chain operating from the basic 100-ke frequency standard and consists of two integral strips. The first of these strips operates directly from the 100-ke crystal standard and consists of a series of tuned

multiplier stages which produce an output signal of 9.6 Mc. This output serves as a locally injected signal for the second mixer and also drives the second high-frequency multiplier strip. This latter multiplier strip consists of several tuned multiplier stages of which the last tripler stage is a pencil triode mounted in a coaxial cavity. This last stage provides local oscillator power for the crystal mixer at approximately 1,036 Mc. The fourth component of the receiver is a 9.675-Mc IF strip. This strip consists of several single-tuned stages of relatively conventional design. The output of this strip is fed into a push-button attenuator with five attenuation settings: 0, 3, 5, 20, and 40 db. The 9.675-Mc output from this strip is fed to the second mixer where it is heterodyned with the 9.6-Mc local injection signal previously mentioned in the multiplier chain. The 75-ke intermediate frequency from this second mixer is fed into the second and final IF strip. The narrow band of 500 cycles is attained in this final strip. Carefully designed double-tuned stages are used to obtain a flat-top response curve with a high skirt selectivity. The detector circuit is built into the last stage of the 75-ke IF amplifier. An automatic volume control circuit designed to provide a linear output versus decibel ratio of input signal is included in this strip. Deviation of the desired signal within the narrow bandwidth can be monitored by a high Q, parallel tuned

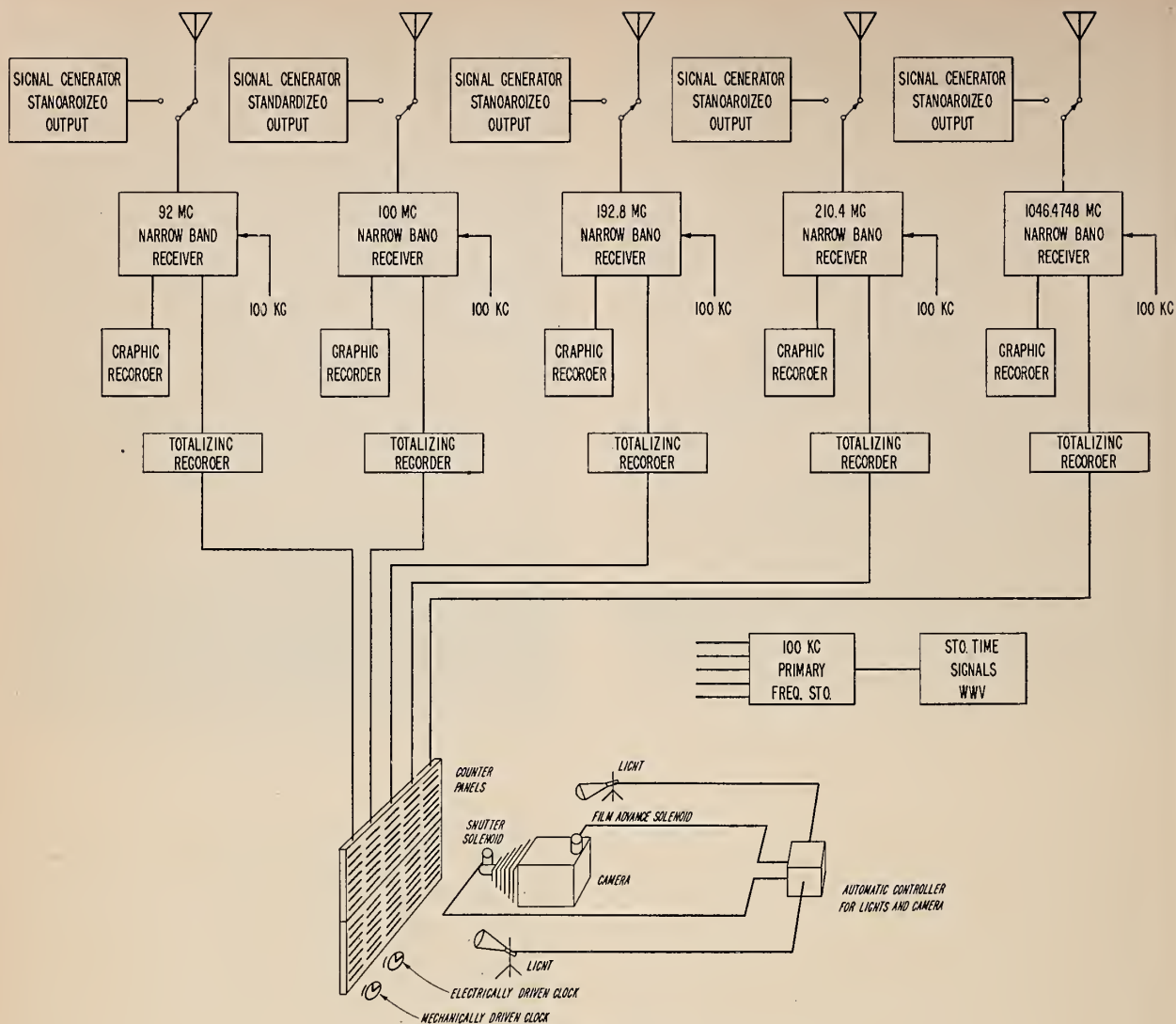


FIGURE 14. Block diagram of fixed recording site.

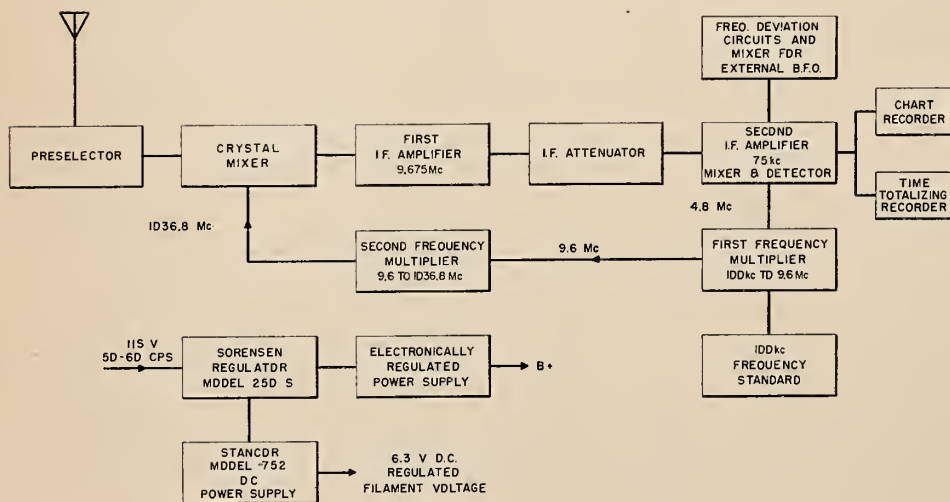


FIGURE 15. Block diagram of 1,046.475-Mc narrow band recording receiver.

circuit, adjustable over a range of plus or minus 500 cycles from the 75-kc center frequency. The last component of the receiver consists of two electronically regulated plate voltage supplies and a filament voltage supply. The IF amplifiers are operated from one plate voltage supply, and the multipliers and frequency deviation circuits are operated from the other. All filaments in the entire system are operated from a regulated d-c voltage supply.

b. Very-High Frequency Receivers—92, 100, 192.8, and 210.4 Mc

The VHF receivers were constructed particularly for use in this program. Special features are utilized to improve gain and frequency stability, and to obtain a very narrow recording channel bandwidth. They are of a triple superheterodyne type, the frequency for oscillator injection voltages being controlled by the same 100 kc primary frequency standard as is employed for the 1,046-Mc receiver. The receivers are identical for each of the frequencies from 92 to 210.4 Mc with the exception of the preselector preamplifier and the first crystal oscillator multiplier circuits. The transmitter frequencies were chosen for adequate separation of all fundamental and harmonic frequencies, and so that suitable receiver-oscillator frequency multiplication factors could be employed. Similar consideration dictated the choice of the replacement frequencies of 230 and 236 Mc which permitted a relatively simple conversion procedure in the changeover of the receivers. The overall effective narrow bandwidth of approximately 1 kc is obtained in the 200-kc third intermediate frequency amplifier which has associated with it a discriminator for determining that the transmitter and receiver are tuned to the same frequency. The 200-kc final intermediate frequency was selected so the second harmonic of the primary frequency standards, which is adjusted to 100 kc by comparing it with WWV, may be used to calibrate the receiver discriminator circuit. Figure 16 is a block diagram of the VHF receivers.

For use at the close-in receiving sites, and for mobile measurements, wideband FM receivers are employed which are crystal controlled and have an effective bandwidth of approximately 200 kc for the 100-Mc band, and 50 kc for the 200-Mc band.

c. Special Receiving Equipment

In order to observe and record rapid and within-the-hour signal variations at the receiving sites within the optical horizon, which are small in magnitude as compared to the steady space-wave component, a combination of a special gain-stable receiver and a differential voltage recorder is employed. Following is a brief description of the components of this special recording chain, a block diagram of which is shown in figure 17.

Gain-stable receiver type GS-2. This receiver was developed at the National Bureau of Stand-

ards. Its basic design principles were described by Boggs [3]. Figure 18 shows a block diagram of the receiver for operation on a frequency of 30 Mc which is used as one of the intermediate frequencies of the special recording system.

The 30-Mc RF amplifier is of the cascode type employing triodes and d-c stabilization to improve its gain stability. A large cathode resistor is used for each tube with the grids returned to a positive voltage. Under normal operating conditions the cathode is slightly more positive which tends to maintain a constant cathode current, and thereby a more constant transconductance.

The mixer employs two stages of IF amplification in conjunction with the mixer "couple". For gain stability, negative feedback at the 450-kc intermediate frequency is applied to the mixer cathode from the cathode of the second IF amplifier stage. The local oscillator is crystal-controlled, and a clamping circuit at the output of the oscillator maintains a constant injection voltage to the mixer stage.

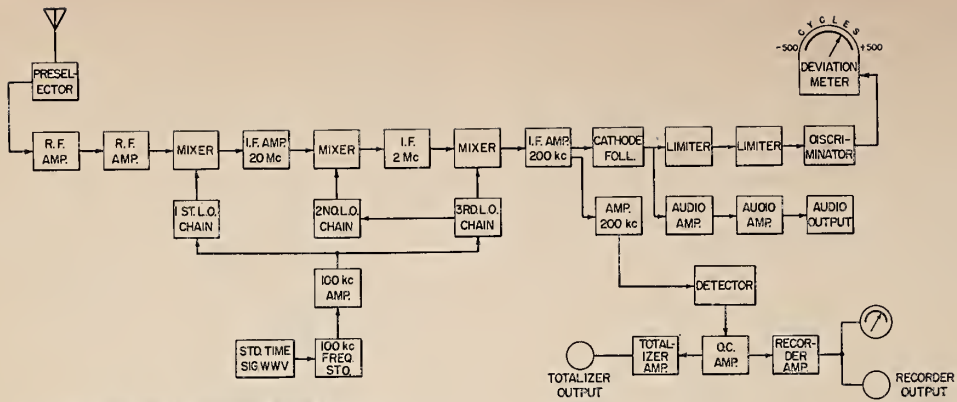
The IF amplifier consists of two couples, each of which contains two stages with negative IF feedback from the output of the second amplifier to the cathode of the first. The gain of the two IF couples is approximately 5,300.

Since negative feedback is used in this receiver in the mixer and IF amplifier stages, no suitable AVC system is available as a basis for obtaining a logarithmic response. Therefore, it is necessary to employ a logarithmic attenuator outside of and separate from the feedback loops. Use is made of the fact that the cathode impedance of a tube varies approximately inversely as the tube transconductance. The transconductance may be controlled by the tube bias. Thus, if the tube bias is supplied in a manner similar to a conventional AVC system, the cathode impedance may be made to vary over a wide range as a function of the input voltage. The two-stage attenuator used gives a logarithmic control over approximately 60 db.

The detector is a conventional diode circuit. An additional large condenser can be switched into the detector output in order to record the average input voltage. The output amplifier driving the recording milliammeter is a d-c bridge arrangement, which is self-compensating for small changes in the supply voltages. The output current is independent of the plate supply voltage as long as the plate resistance remains constant.

This receiver also contains a frequency deviation circuit in order to indicate small changes in the local oscillator or input radio frequency. It consists of a limiter followed by a limiter-discriminator with a d-c microammeter in the output bridge circuit. The meter scale is directly calibrated for deviations up to $\pm 1,500$ c/s.

The over-all gain stable characteristics of the receiver are shown in figure 19, which indicates



LOCAL OSCILLATOR FREQUENCIES (Mc)

SIG. FREQ.	LOCAL OSC.	INPUT	MULT. FREQ.	OUTPUT
92	1 ST.	0.1	0.1, 0.3, 0.9, 1.8, 9, 18, 36, 72	72
100	1 ST.	0.1	0.1, 0.9, 2.5, 5, 15, 30, 60, 120	120
192.8	1 ST.	0.1	0.1, 0.3, 0.9, 2.7, 5.4, 10.8, 21.6, 43.2, 86.4, 172.8	172.8
210.4	1 ST.	0.1	0.1, 0.3, 0.9, 1.8, 3.6, 7.2, 14.4, 28.8, 57.6, 115.2, 230.4	230.4
92, 100,	2 ND	1.8	1.8, 9, 18	18
192.8, 210.4	3 RD	0.1	0.1, 0.3, 0.9, 1.8	1.8

FIGURE 16. Block diagram of VHF receivers.

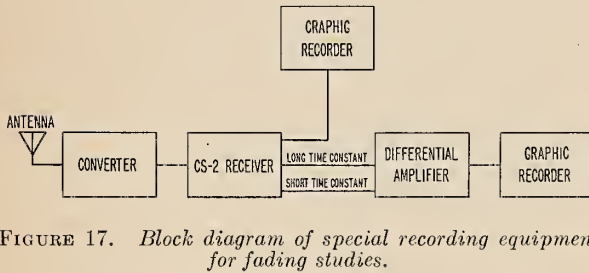


FIGURE 17. Block diagram of special recording equipment for fading studies.

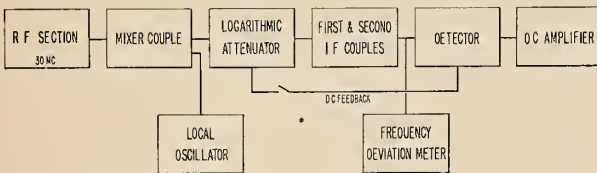


FIGURE 18. Block diagram of GS-2 receiver.

that the heater voltage can drop from nominal 6.3 v to 4.5 v before the over-all gain is reduced by one decibel. Similarly, the plate supply voltage may be reduced to 125 v before the over-all receiver gain drops one decibel. Due to the fixed d-c stabilizing voltage used the supply voltage to the radio-frequency amplifier is held constant.

The over-all noise figure of the receiver with its 6 kc bandwidth is 4 db. Its input impedance is 50 ohms.

Converter. In order to utilize the gain-stable receiver in the Cheyenne Mountain experiments,

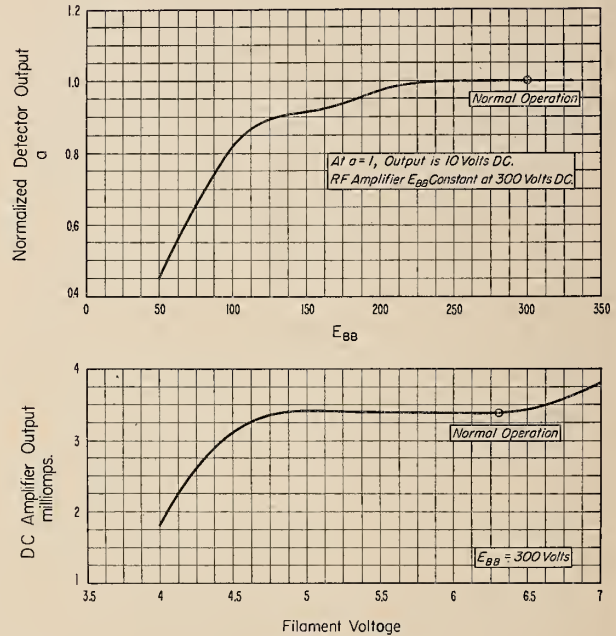


FIGURE 19. Stability characteristics of GS-2 receiver.

a suitable converter has to be employed in order to convert the measured VHF or UHF frequency to the 30-Mc intermediate frequency of the gain-stable receiver. A unit for the utilization of the 100-Mc signals has been built and similar units for the other frequencies will be employed.

The 100-Mc converter employs a miniature twin triode with its plates connected in parallel as the

mixer. The 100-Mc signal voltage is supplied to one of the grids, and the 70-Mc local oscillator injection voltage to the other. The plate circuit is tuned to the 30-Mc intermediate frequency which is the frequency to which the following GS-2 receiver is tuned. An untuned loop is used for output coupling, providing a VSWR better than 1.2 at the 50-ohm output impedance. The converter is matched to the 50-ohm 100-Mc antenna with a tuned auto transformer.

The converter uses a crystal controlled local oscillator at 23.333 kc followed by a tripler stage which consists of a twin triode with its grid connected in push-pull and the plates in parallel. Constant injection voltage to the mixer is maintained by a clamping circuit on the multiplier output.

The over-all noise figure of the combination of converter and type GS-2 receiver is approximately 8 db.

Differential voltage recorder. The differential voltage recorder compares the difference of an average and an instantaneous voltage, amplifies this difference, and supplies it to a recorder. These two voltages are obtained from specially installed output circuits of the GS-2 gain-stable receiver. One of these is the long time constant average output voltage of the detector which is proportional to the average input signal level, while the other circuit is connected ahead of the long time constant filter to obtain a voltage proportional to the instantaneous signal level.

Figure 20 shows a block diagram of the differential voltage recorder. For each input a cathode follower circuit is provided in order to insure high input impedance, and complete isolation. Both signals (the average and the instantaneous) are fed through a double-pole, double-throw synchronous chopper. An a-c output voltage is obtained from the chopper which is equal to the difference between the average and instantaneous signals. This voltage is amplified, synchronously detected for determination of the algebraic sign of the difference voltage, and applied to a bridge-type d-c recorder amplifier. The differential recorder is calibrated by the use of an internal calibrating voltage.

Since the average signal produced by the long-time-constant circuit controls the logarithmic

attenuation of the GS-2 receiver, the short-term variations are linear about the long time average. A calibration of the differential voltage recorder is obtained by the use of the following relation:

$$E_i = E_{av} \frac{V_{av} - V_D}{V_{av}}$$

where

E_i = Instantaneous radio-frequency input voltage to the receiver.

E_{av} = Average radio-frequency input voltage to the receiver.

V_{av} = Average d-c detector voltage output from the long time constant circuit for E_{av} input to the receiver.

V_D = Differential voltage between the long and short-time-constant detector outputs with its algebraic sign observed. (The average short-time-constant detector output equals the long-time-constant output.)

Also, the differential voltage D_{FS} for full scale differential recorder deflection is given by the following relation:

$$D_{FS} = E_{av} \frac{V_{FS}}{V_{av}}$$

where V_{FS} is the d-c calibration voltage for full-scale deflection of the differential recorder.

d. Recording Devices

The conventional type of data-recording equipment used with all receivers consists of a clock-driven chart recorder and a 10-channel time-totalizing recorder. The time totalizer recorder, driven from the 0 to -10 v AVC output from each receiver, consists of 10 channels, each of which includes a d-c amplifier, and a bistable multivibrator that actuates a fast acting relay. The relay in turn operates a motor which drives a revolution counter. The multivibrators are adjusted to operate the relays at various levels of input voltage from the d-c amplifiers. Thus, the revolution counter will indicate the total time that the signal exceeds a preset level. Hourly readings of the counters are made with an automatically actuated 35-mm camera. A typical recording arrangement is illustrated in figure 14.

3.4. Meteorological Facilities

The Cheyenne Mountain meteorological project consists of two phases: a low-level system for determining at a fixed site the important radio meteorological phenomena, and a portable method of determining these phenomena along the path by utilizing aircraft and radiosonde. The first phase includes a complete meteorological installation at the Haswell site as shown in the block diagram of

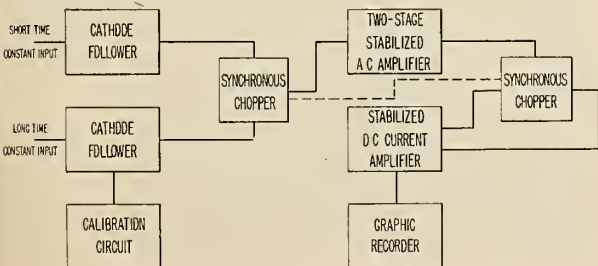


FIGURE 20. Block diagram of the differential voltage recorder.

figure 21. A 500-ft tower has been instrumented to record unattended continuously the various parameters, such as refractive index, wind direction and velocity, scale of turbulence, temperature, pressure, relative humidity, and solar radiation.

The refractive index of the atmosphere can be measured by the use of a recently developed instrument known as the microwave refractometer. The National Bureau of Standards microwave refractometer [4] is an instrument designed to measure changes in the resonant frequency of a cavity resonator. This frequency is a function of the refractive index of the air admitted to the cavity and the cavity dimensions. As indicated in the block diagram (fig. 22) the frequency of a klystron oscillator is swept through the resonant frequencies of the test cavity and a sealed reference cavity. A pair of video pulses is generated by the detectors associated with the two cavities, and the phase difference between these pulses is recorded. Any variation in refractive index of the air in the test cavity changes its resonant frequency and the phase of its pulse with respect to that produced by the reference cavity. The frequency used is in the neighborhood of 9,000 Mc, and the equipment has a long-term stability of approximately one N-unit of refractive index. Figure 23 shows photographs of various components of this microwave refractometer.

Precision recording instruments, together with standard weather bureau devices, are utilized in conjunction with the refractometer measurements to supply the other necessary meteorological data.

The second phase of this program, as yet in the planning stage, includes the development of a portable refractometer for installation in a high-flying aircraft and the use of radiosonde equipment to obtain essentially the same data along the radio-transmission path as at the Haswell site.

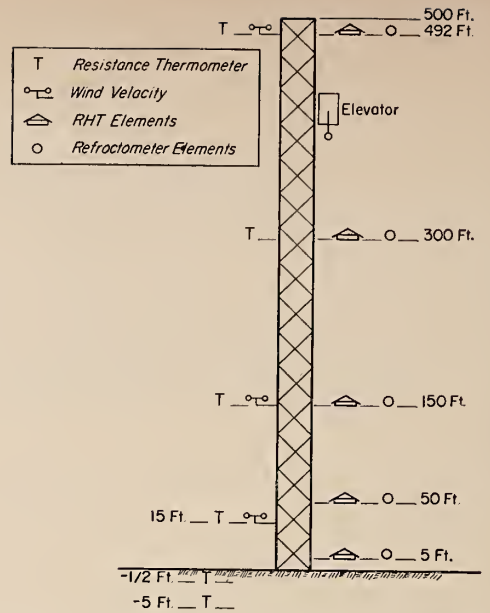


FIGURE 21. Instruments on 500-ft tower at Haswell, Colo.

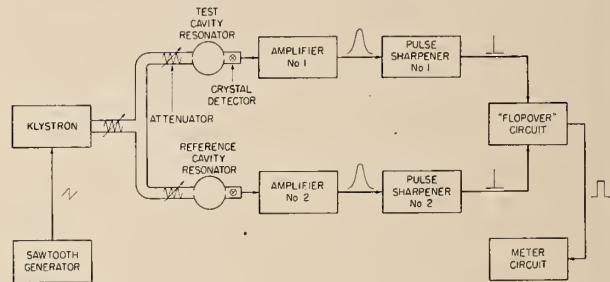


FIGURE 22. Arrangement of components of the refractometer.

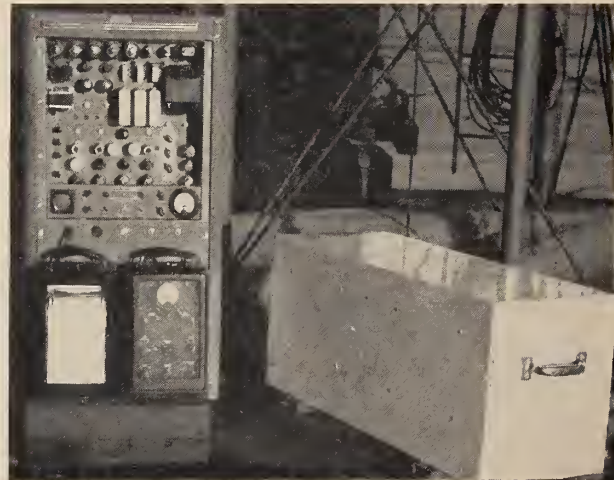
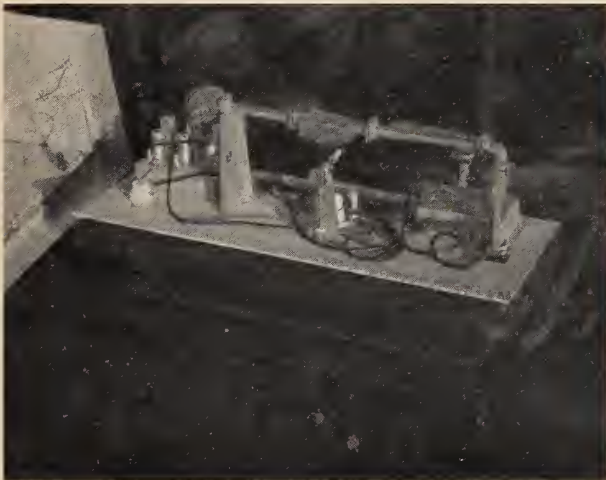


FIGURE 23. Microwave refractometer.

4. Operations

4.1. Transmitter Operations

In order to keep the transmitting equipment in operation continuously it is desirable not only to have operators on duty for 24 hr/day, but also to have qualified maintenance personnel available for servicing if necessary. A compromise has to be made which assures operation as trouble-free as possible with the personnel available. At the summit site the operators are on continuous duty working in 8-hr shifts. The base site is controlled remotely from the summit site by a dialing system that permits the following remote operations: a. Turning on and off filament and plate power of both transmitters; b. reading power level of both transmitters; c. raising and lowering output power d. raising and lowering carrier frequency; and e, turning on and off primary power for the entire base site installation.

Receivers for both base-site frequencies are installed at the summit site, which permit direct monitoring of the carrier frequencies, enabling the operator to make changes if necessary. An automatic fire-extinguishing system protects the unattended base site.

The operator on watch keeps two sets of logs: one for the purpose of transmitter maintenance and operation records, and one for the purpose of aiding the data analysis. This latter log contains only power output and frequency reading for each transmitter, together with on and off periods. The other log contains the usual information pertaining to transmitter operator, e. g., values of grid and plate current of the various amplifier stages. Final power output and frequency are logged every half hour; other data every hour. The transmitter operator makes necessary adjustment in carrier frequency and output power level whenever necessary.

The transmitter output is calibrated at regular intervals. A definite schedule is followed as far as preventive maintenance is concerned, which includes checking the antenna installations and the transmission lines. The frequency is checked against a frequency counter which may be connected to all transmitters by a coaxial switch.

4.2. Receiver Servicing and Calibrations

Although the receiving sites are set up basically for unattended operation, servicing at regular intervals is necessary due to the need for frequent calibration of the receiver output, and due to equipment failures which are unavoidable. Another factor is the frequency of power failures, or substantial fluctuations and surges which occur on the rural power lines. A regular servicing schedule has been set up for the first three receiving sites, which provides for at least four visits per week by qualified personnel at each receiving site.

The Garden City site is attended daily by a man stationed in Garden City. Recording runs at Anthony and Fayetteville have sufficient personnel in constant attendance.

It has been found advisable to install air-conditioning equipment at the four fixed recording sites in addition to a thermostat-controlled heating and ventilating system in order to keep the temperature constant within 10 deg all year round. The equipment is installed in small semiportable shelters on the treeless prairie, and the heating and air-conditioning equipment prevents not only extreme temperature differentials in the interior of the shelters, which causes changes in receiver gain characteristics, but also protects the receiving and associated equipment from failure due to extreme operating temperatures.

Maintenance personnel visiting the fixed recording sites perform essentially the following duties: (1) Inspection of equipment and auxiliary facilities, and seeing that everything is in proper operating condition, (2) performing minor repairs and adjustments if necessary, (3) calibrating the receiver outputs by use of standard signal generators, and (4) changing recorder chart rolls and microfilm spools when necessary.

For the VHF receivers, signal generators are used to calibrate with the calibrations being marked directly on the recorder charts in transmission loss relative to the 2-kw transmitter output power. The 1,046-Mc receivers are calibrated in decibels below 1 mw by specially constructed crystal-controlled signal generators. Whenever time totalizers are employed the levels are set simultaneously with the calibrations to correspond to calibration marks on the charts.

When major repairs on equipment are necessary, the particular piece of apparatus is replaced by a spare, and brought into the laboratory for repair and testing. Signal generators are checked periodically against a common standard located in the laboratory, which basically employs micro-potentiometers, calibrated by accurate galvanometer methods. The primary standard available for the UHF signal generators is a bolometer-type bridge and associated attenuators. The 1,046-Mc signal generators are also checked against each other and the standard periodically.

A log of receiver operation is kept, together with a duplicate record of each calibration. These logs are studied, together with the recordings themselves, in order to determine which data are reliable, and which have to be discarded due to equipment trouble.

The milliammeter graphic chart recorders are operated at a speed of 3 in./hr at the Kendrick and Karval receiving sites. At Haswell the same speed is used for the frequencies in the 100-mc range, whereas double speed (6 in./hr) is used for the higher frequencies due to the increased fading

rate. At the sites far beyond the radio horizon the tapes are run at speeds ranging from 0.75 to 6 in./min in order to permit accurate fading-rate analysis; and a check of the time-totalizing equipment. Wherever time totalizers are employed the counter dials are photographed every hour, together with a clock-face showing the time and other pertinent information. Figure 24 shows a typical microfilm frame indicating location, day, time, and calibration for each level of each receiver output. The camera equipment and associated flood lights are operated by relays.

4.3. Meteorological Observations

The instruments installed on the 500-ft tower at Haswell make it possible to record continuously the following data: a, Wind velocity and direction by anemometers at the 15-, 150-, and 500-ft levels; b, temperature and relative humidity at the 5-, 50-, 150-, 300-, and 500-ft levels; c, additional temperature measurement at 1 and 3 ft beneath ground levels; d, barometric pressure at the surface level, and e, direct measurements of the refractive index by use of the microwave refractometers, which

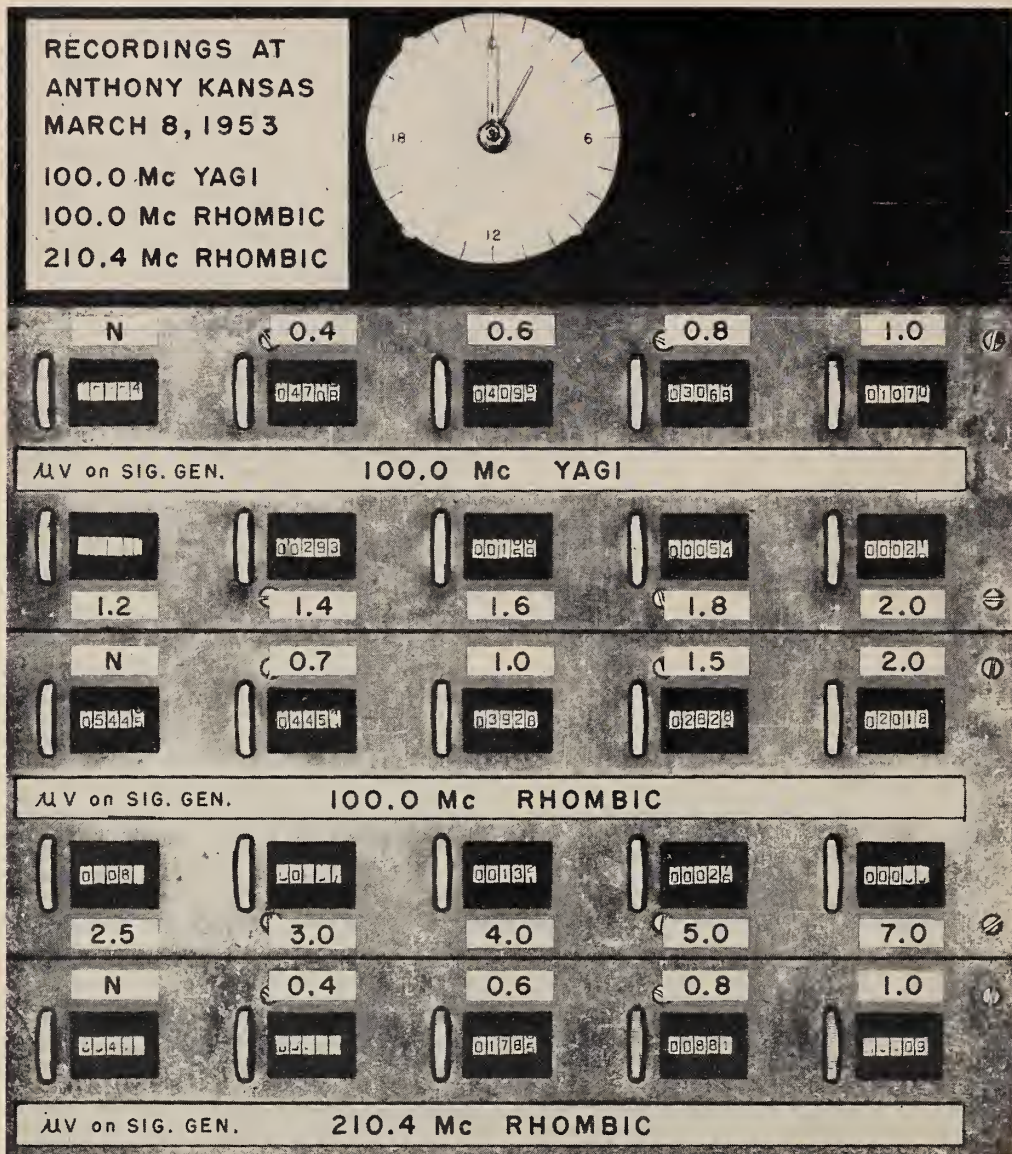


FIGURE 24. Sample of microfilm frame.

will be installed at the 5-, 50-, 150-, 300-, and 500-ft levels as soon as components for all locations are available.

In addition to continuous measurements at fixed levels, it was planned to mount a microwave refractometer on the elevator and record the refractive index as a continuous function of height while making runs up and down the entire height of the tower. However, so far it has not been possible to overcome operational difficulties in this procedure.

Other short-term measurements will provide for the operation of refractometers at various levels relative to a fixed installation in order to provide

data for a study of turbulence.

Conventional instrumentation to record temperature, pressure, and relative humidity at the 5-ft level is provided at the Kendrick and Karval sites, and may be installed where desired for any specific tests.

Until preliminary results become available from the instruments installed, so far it has been considered impracticable to establish definite operational procedures in the meteorological program. The results of the radio-propagation experiments will also be of considerable importance in the study of what kind and what amount of meteorological data are desired.

5. Data Analysis

5.1. General

The propagation mechanism of VHF and UHF radio waves is closely related to the properties of the troposphere. The study of expected changes in propagation conditions is, therefore, quite similar to the task of predicting weather conditions. Two approaches to the analysis of wave propagation data may be taken. Radio measurements may be correlated with simultaneous meteorological observations, and thereby radio wave propagation characteristics may be determined as a function of the behavior of physical properties of the atmosphere. It is also possible to study the behavior of radio transmission loss or field strength in itself on a statistical basis in order to estimate the expected variations significant for operational purposes. In our studies these two methods of approach are developed in such a way as to complement each other.

It is necessary to have a picture of the propagation mechanism before attempting to evaluate the data. Basically, the transmission loss over any given transmission path consists of a component dependent only on path length and frequency, and components dependent also on terrain features and the properties of the atmosphere. For a fixed transmission path over which continuous long-term measurements are carried out, only the components dependent on the properties of the atmosphere need be considered variable.

It is beyond the scope of this Circular to develop theories of wave propagation applicable to VHF and UHF transmissions. Certain basic definitions, however, are included in order to facilitate an understanding of the procedures followed in data analysis.

Transmission loss is defined as the ratio of power supplied to the terminals of a loss-free transmitting antenna to the power available at the terminals of a loss-free receiving antenna, expressed in decibels. Basic transmission loss is defined as the transmission loss which would be present if both antennas were isotropic.

Actually only the transmitter power output and the power input to the receiver terminals can be measured accurately. Transmission loss over a

given path, therefore, is determined by subtracting transmission line losses from the ratio of transmitter output power to receiver input power (expressed in decibels). Basic transmission loss may be determined from measured transmission loss by adding the path antenna gain expressed in decibels, a quantity which is usually only slightly smaller than the sum of the free space gains of the transmitting and receiving antennas. Under the assumption that the free space antenna gains are realized, basic transmission loss is simply the algebraic sum of the transmission loss and the gain values (in decibels) of the transmitting and receiving antennas. Basic transmission loss under this assumption also may be defined as the sum of free space loss and a component termed attenuation relative to free space, both expressed in decibels. This latter component is the one which is taken to be variable; in practice, of course, only the overall transmission loss can be measured and the basic transmission loss and the attenuation relative to free space are derived quantities.

The above discussion may be represented by several simple equations:

L'_m = The ratio, expressed in decibels, of the transmitter power output to the power available to the receiver.

L_m = Transmission loss as defined above.

$L_t + L_r$ = Transmission line and antenna losses for the transmitting and receiving systems.

L_B = Basic transmission loss.

L'_B = Basic transmission loss determined on the assumption that the free-space antenna gains are realized.

B = Free space loss (which is also the basic transmission loss in free space).

A = Attenuation relative to free space.

A' = Attenuation relative to free space under the usual assumption that the free-space gains are realized.

G_p = Path antenna gain, which is equal to or somewhat less than the sum ($G_t + G_r$) of the free-space gains of the transmitting and receiving antennas.

All of the above quantities are expressed in decibels, and the following equations result:

$$L_m \equiv L'_m - (L_t + L_r)$$

$$L_B \equiv L_m + G_p$$

$$L'_B \equiv L_m + G_t + G_r$$

$$B = 20 \log \left(\frac{4\pi d}{\lambda} \right) = 20 \log d + 20 \log f + 36.581$$

$$A \equiv L_B - B \equiv L_m + G_p - B$$

$$A' \equiv L'_B - B \equiv L_m + G_t + G_r - B,$$

where d is the path distance in miles, and f the frequency in megacycles [5].

The quantity A will contain different components depending on the propagation mechanism involved. For propagation within the radio horizon it may be calculated by determining the gain or loss introduced by combining two or more rays in their proper phases depending on their relative path lengths, as well as additional components dependent on terrain roughness. Relative path length is also a function of the refractive properties of the atmosphere, and this is one of the variables studied by continuous long-term measurements. For propagation in the region around and slightly beyond the radio horizon, attenuation relative to free space may be calculated by the diffraction theory, with appropriate allowance for the influence of terrain roughness. For propagation far beyond the radio horizon, scattering by atmospheric turbulence is considered to have a predominant effect on the attenuation.

It has been found convenient to express the results of the measurements in terms of basic transmission loss which, as shown above, contains constant components depending on total path length and frequency in addition to the variable attenuation component.

Variations in transmission loss may be classified arbitrarily as short term and long term. Until such time as experimental evidence makes a revision to a still shorter interval desirable, short-term variations will be defined as variations occurring within 1 hr. Fading range has been defined as the ratio of the transmission losses (in decibels) exceeded for 10 percent and 90 percent of 1 hr. The fading rate, corresponding to a particular interval of time (usually taken to be 1 hr.), is defined as one-half the number of times the instantaneous transmission loss (recorded signal level trace) passes through the median level for the interval under consideration, divided by the length of the interval expressed in seconds. The fading period for this interval of time is simply the reciprocal of the fading rate.

The study of long-term variations considers the hourly median value of transmission loss as the basic unit. This hourly median value of transmission loss exhibits diurnal and month-to-month (seasonal) variations. It has been found convenient to study the cumulative distribution of hourly median values over monthly or other periods, and obtain from these distributions the interdecile range of hourly medians as a measure of the expected variations. The interdecile range, in turn, is defined as the ratio (in decibels) of the transmission loss values exceeded by 10 percent and by 90 percent of all hourly medians comprising the distribution studied.

Measurements obtained so far at all fixed receiving sites have shown that values for monthly or longer periods of hourly median levels of transmission loss expressed in decibels, usually approximate a normal distribution. Short-term variations, however, are characterized by a distribution of levels which approach the theoretical combination of a steady signal plus a Rayleigh-distributed signal. Thus the received power over a tropospheric propagation path may be considered to consist of a steady, or slowly varying component, plus the vector sum of a large number of components of comparable amplitude and random relative phase. These characteristics are utilized in classification of data and plotting on specially designed graph paper. Samples will be shown in the course of subsequent discussions.

5.2. Recording Charts

The analysis of recording charts is performed by manual scaling. For each desired time interval the median or other transmission loss level is determined by placing a straight edge parallel to the horizontal guidelines on the charts and moving it to a position where the desired percentage level of recording trace above and below the guideline is obtained. This position is converted into transmission loss, L'_m , by use of a pertinent chart calibration, and tabulated. Typical chart recordings as obtained during 1953 are shown on figures 25, 26, and 27. Figure 25 shows the 100-Mc signal at Kendrick, Karval, and Haswell recorded during the evening hours of April 23, 1953, at a chart speed of 3 in./hr. Figure 26 shows a comparison of various frequencies at Karval at the same chart speed for the early morning hours of April 21, 1953. Figure 27 shows a comparison of various frequencies at Garden City for midmorning of March 8, 1953, illustrating the rapidity of fading at distances far beyond the radio horizon and the dependence of fading rate on frequency. The chart speed in this instance is 1.5 in./min. From a record of this kind, fading range and fading rate may be determined quite accurately by manual scaling, although this process is slow and tedious.

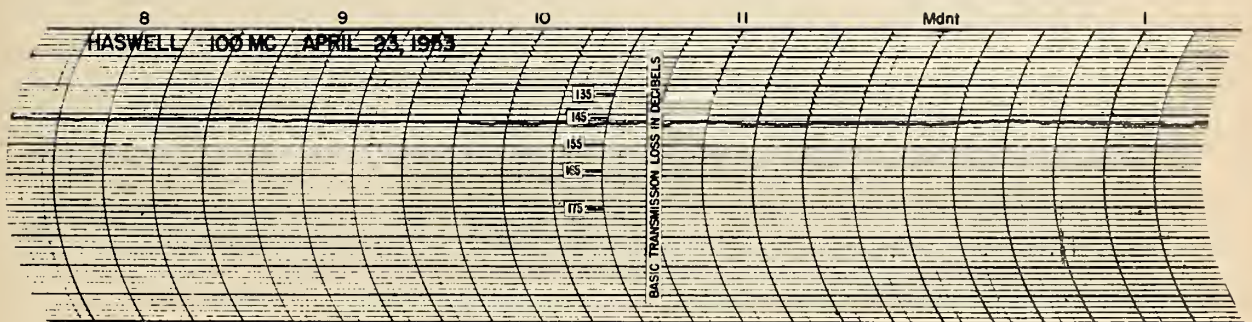
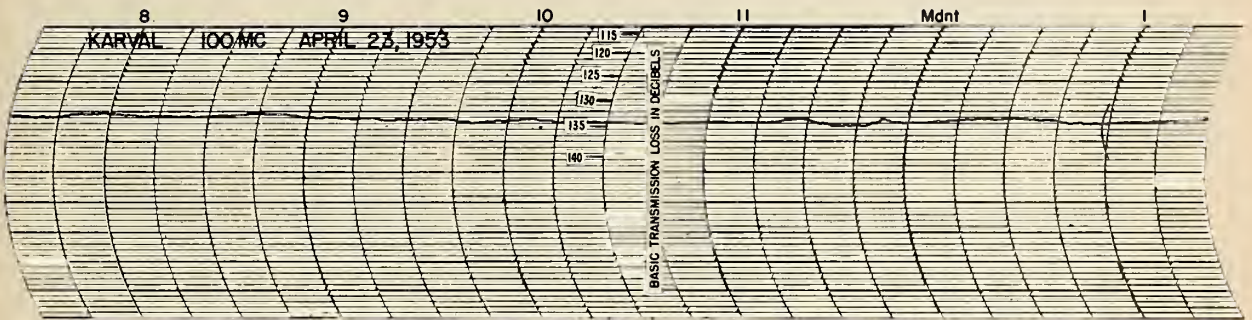
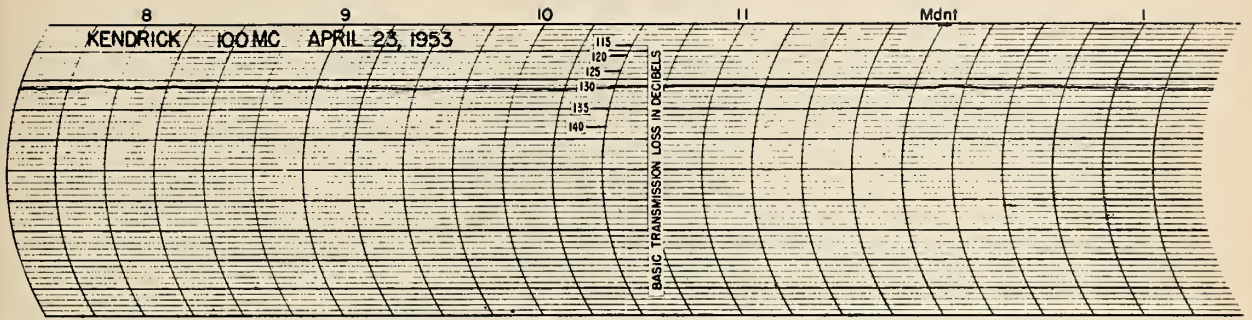


FIGURE 25. Recording chart samples showing 100 Mc at Kendrick, Karval, and Haswell.

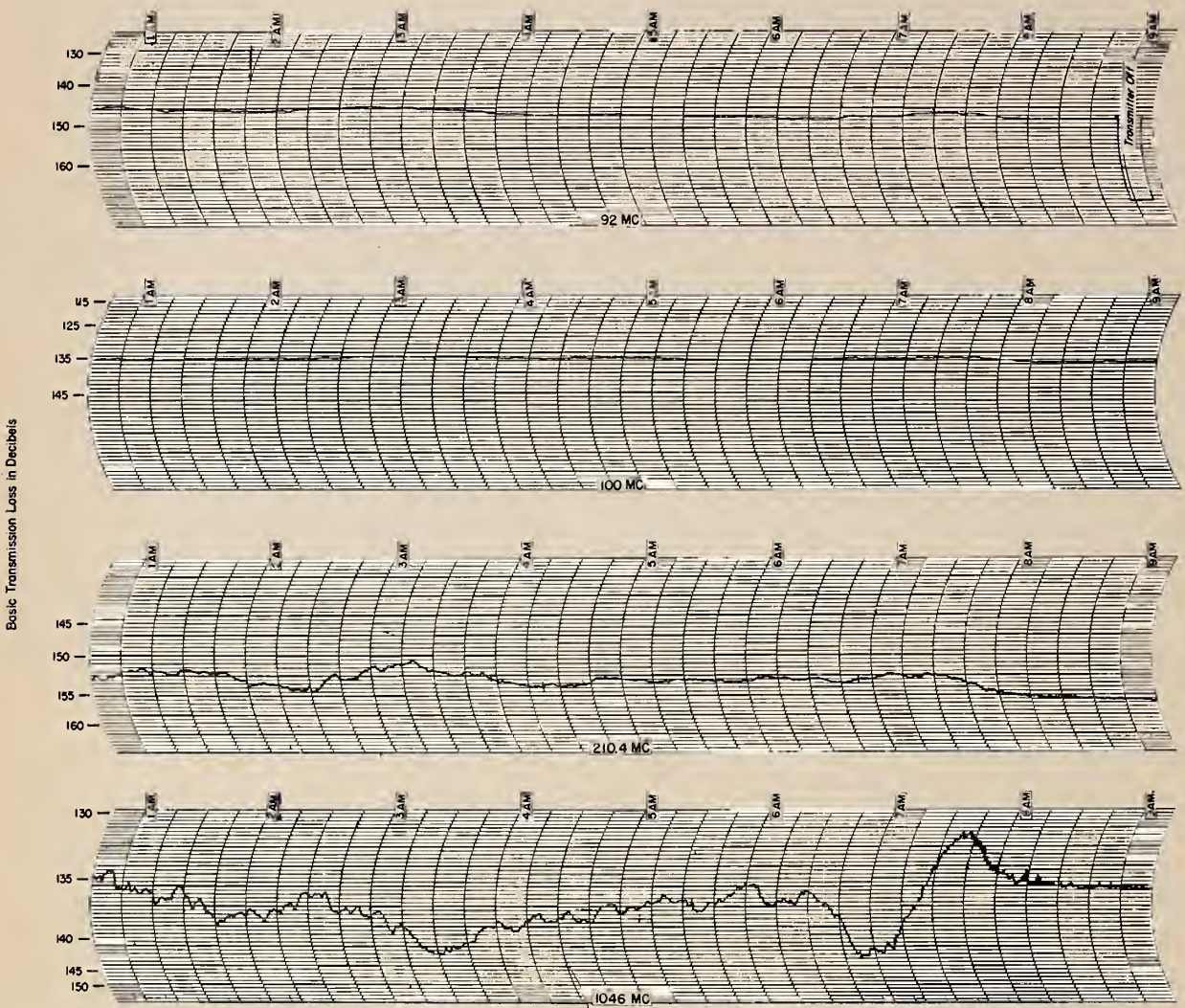


FIGURE 26. Recording chart samples showing all frequencies at Karval, April 21, 1953.

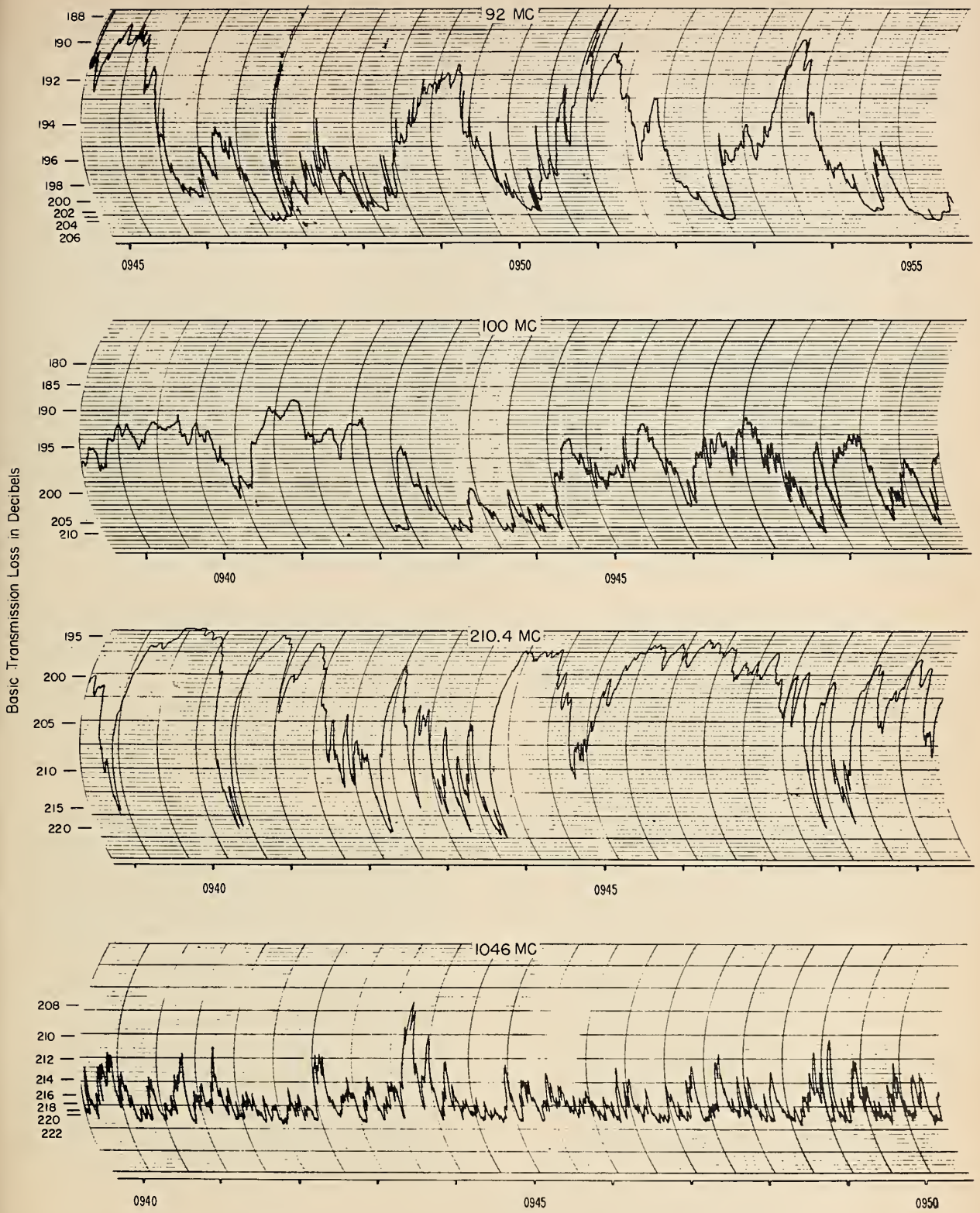


FIGURE 27. Recording chart samples showing all frequencies at Garden City, March 8, 1953.

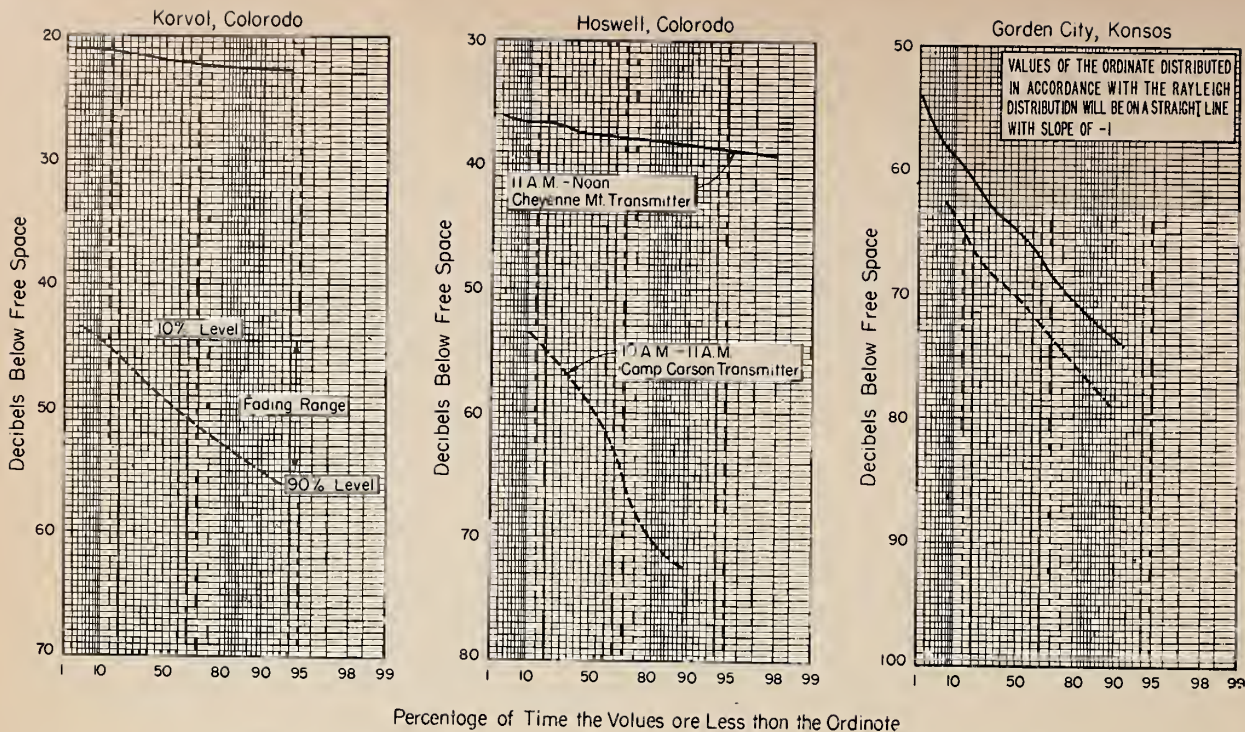


FIGURE 28. Sample of distributions of instantaneous signal levels, August 9, 1952.

100 Mc.

5.3. Time Totalizer Data

The appearance of a microfilm frame showing time totalizer data at Anthony, Kans., is illustrated in figure 24. For each frequency, differences in counter indication on successive frames are tabulated and, with the aid of calibrations indicated on the face of the counter panel, these differences are converted into the percent of time each level was exceeded during the period between successive frames (usually 1 hr). The resulting distributions of level versus percent of time are plotted on graph paper which is designed in such a way that the Rayleigh-distributed variable in decibels will appear as a straight line having a slope of -1 . If charts are analyzed for the distribution of signal levels within the hour the same procedure in plotting is followed. In both cases the median or any other percentage value of transmission loss is read directly from the graph and entered in an appropriate tabulation for further use. Figure 28 shows samples of distributions of instantaneous signal levels determined from time totalizers as well as chart records, illustrating conditions within and beyond the radio horizon.

5.4. Study of Long-Term Variations

A tabulation of hourly median values of transmission loss for any particular frequency at any particular site contains up to 744 individual hourly medians per month of record. They are usually read off the recording charts to the nearest one-

tenth decibel. In order to study the variations over the entire monthly period, a cumulative distribution of all hourly median levels is computed and plotted on logarithmic probability graph paper. Prior to the computation of the distribution, the values are rounded off to the nearest one-half decibel. Figure 29 shows a sample illus-

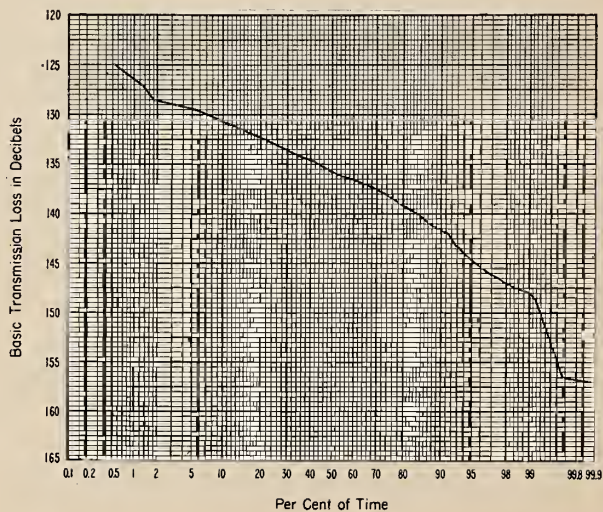


FIGURE 29. Sample distribution of hourly medians, Cheyenne Mountain-Karval path, 1,046 Mc, May 1953.

459 hours

trating the distribution of 459 hourly medians of the transmission loss for Karval during May 1953 on 1,046 Mc. The monthly median and the interdecile range as well as any other percentage values may be read directly from a distribution of this kind.

Diurnal variations of hourly medians are obtained from distributions taken over 3-hr periods rather than for each individual hour. The day is divided into eight 3-hr periods, and cumulative distributions of hourly medians are obtained for each period for each month of data. From these cumulative distributions the median and the interdecile range for each of the eight 3-hr periods are determined in the same way as these quantities were obtained from the overall monthly distribution. The diurnal variation of hourly median and interdecile range are then plotted versus time of the day.

Figure 30 shows a sample of cumulative distributions of 92-Mc hourly medians of the transmission loss for Haswell during March 1953 for the time periods midnight to 3 a. m. and noon to 3 p. m., indicating the observed difference of the distributions of hourly medians between day and nighttime. Figure 31 shows a sample of diurnal variations of the hourly medians obtained by the method described above, illustrating the 92-Mc data at five sites received during February of 1953. The diurnal variations have also been plotted in a different way. Figure 32 shows a scatter diagram of 1,046 Mc hourly medians for Haswell during April 1953. Each point represents one hourly median, plotted at the time of the day and at the level it occurred. From this diagram the level exceeded by any desired percentage of medians may be found directly by counting, and on the sample the 10-, 50-, and 90-percent variations are indicated.

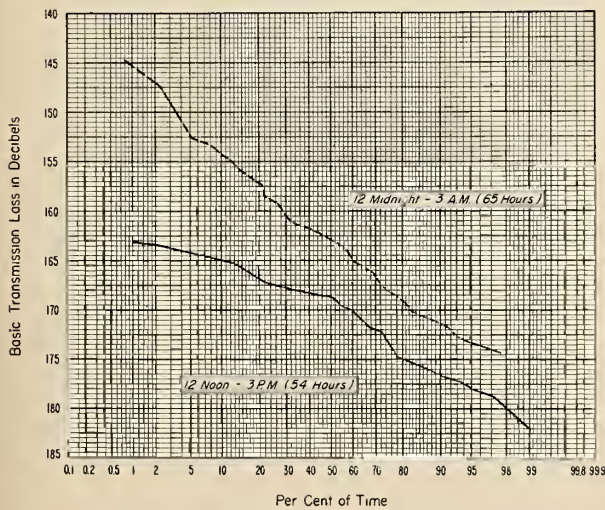


FIGURE 30. Sample distribution of hourly medians, Cheyenne Mountain-Haswell path, 92 Mc, March 1953.

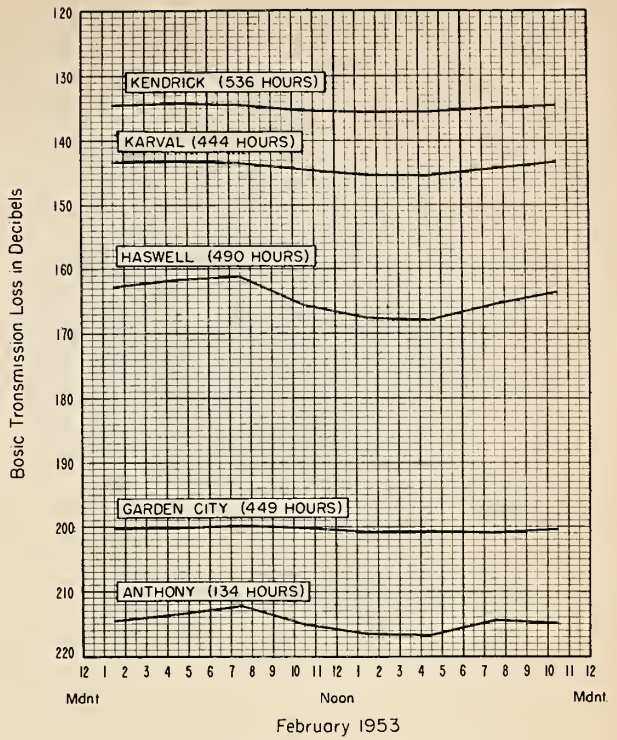


FIGURE 31. Diurnal variations of hourly medians, 92 Mc

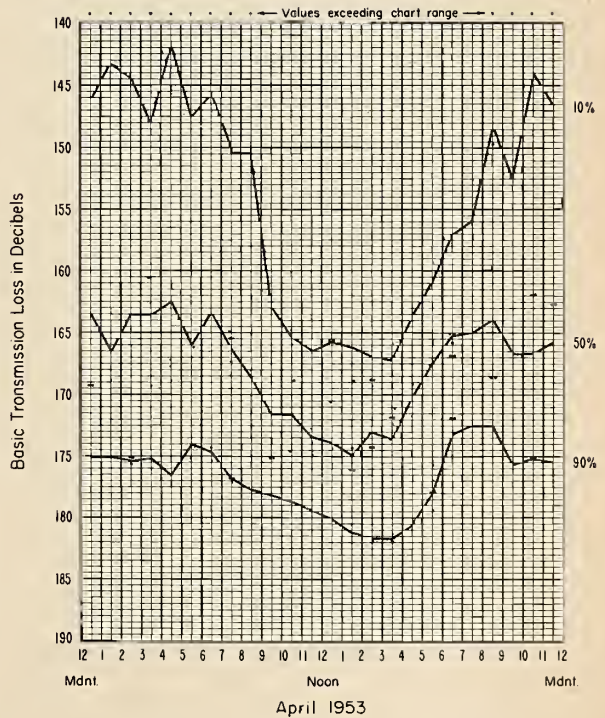


FIGURE 32. Scatter diagram of hourly medians, Haswell, 1,046 Mc

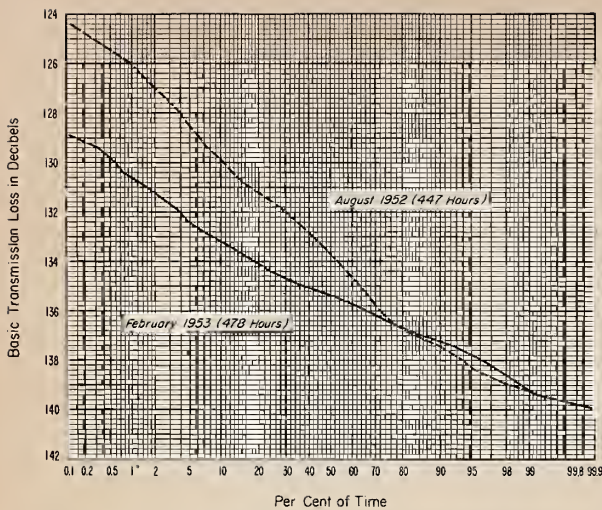


FIGURE 33. Sample distribution of hourly medians, Cheyenne Mountain-Karval path.

100 Mc

Month-to-month variations of any of the data derived from the distributions have also been established, as the overall monthly distributions vary considerably from month to month. Figure 33 shows a comparison of the overall monthly distribution of hourly medians for August 1952 and February 1953 using 100-Mc data at Karval.

5.5. Study of Short-Term Variations

The plot of distributions of signal levels within the individual hours (fig. 28), which is obtained from the time totalizer record or graphic millimeter charts as described above, provides the basic information for the study of fading range, as the hourly median and the fading range may be read from the graph directly. The fading range as defined above can be obtained directly from the charts by counting the number of signal excursions above the median. Diurnal and month-to-month variations of fading range and fading rate, as well as their dependence on frequency, angle θ , or any other desired parameter, may then be studied and evaluated in a similar way as the hourly medians. Figure 34 shows a sample of the diurnal variations of fading range comparing three frequencies received at Anthony during August 1952. The average fading range is obtained from the average distributions of instantaneous signal levels, samples of which are shown in figures 35 and 36 for Haswell and Garden City, also during August 1952.

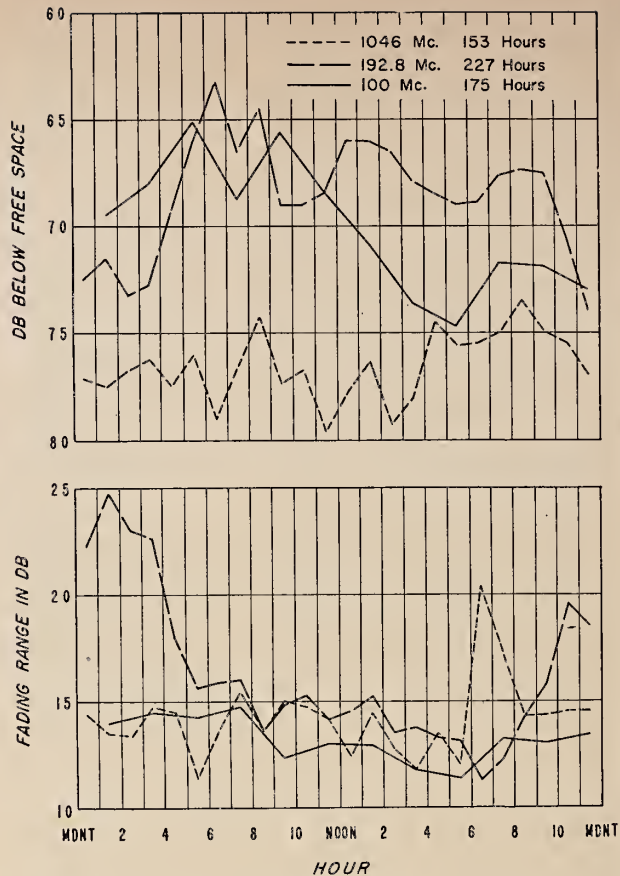


FIGURE 34. Diurnal variation of median attenuation and of median fading range.

Cheyenne Mountain to Anthony, Kans., August 1952.

5.6. Study of Prolonged Space-Wave Fadeouts on 1,046 Mc

In the course of the Cheyenne Mountain measurements program it has been found that the 1,046-Mc signal as received at Karval (just within the radio horizon of the transmitter) exhibits large fluctuations in intensity which are far too long to be classified as short-term fading. The signal occasionally drops 15 to 20 db below the monthly median value for periods ranging from a few minutes to several hours. In order to illustrate the method of systematically evaluating these fadeouts the following procedure is described: for each observed occurrence of a fadeout its total period as well as the period certain levels below the monthly median are reached are tabulated. The simultaneous behavior of the 1,046-Mc field at Kendrick (well within the radio horizon), and Haswell (somewhat beyond the radio horizon) is

also studied for comparable fadeouts. A concise definition of a fadeout at Karval specifies a duration of at least 1 min, and a drop in signal level to at least 5 db below the monthly median. Figure 37 shows a typical Karval fadeout together with

simultaneous records of the 1,046-Mc signal at Kendrick and Haswell, as recorded on charts. It is worth noting that this phenomenon has not been observed on lower frequencies. The 1,046-Mc trace on figure 26 also contains a fadeout oc-

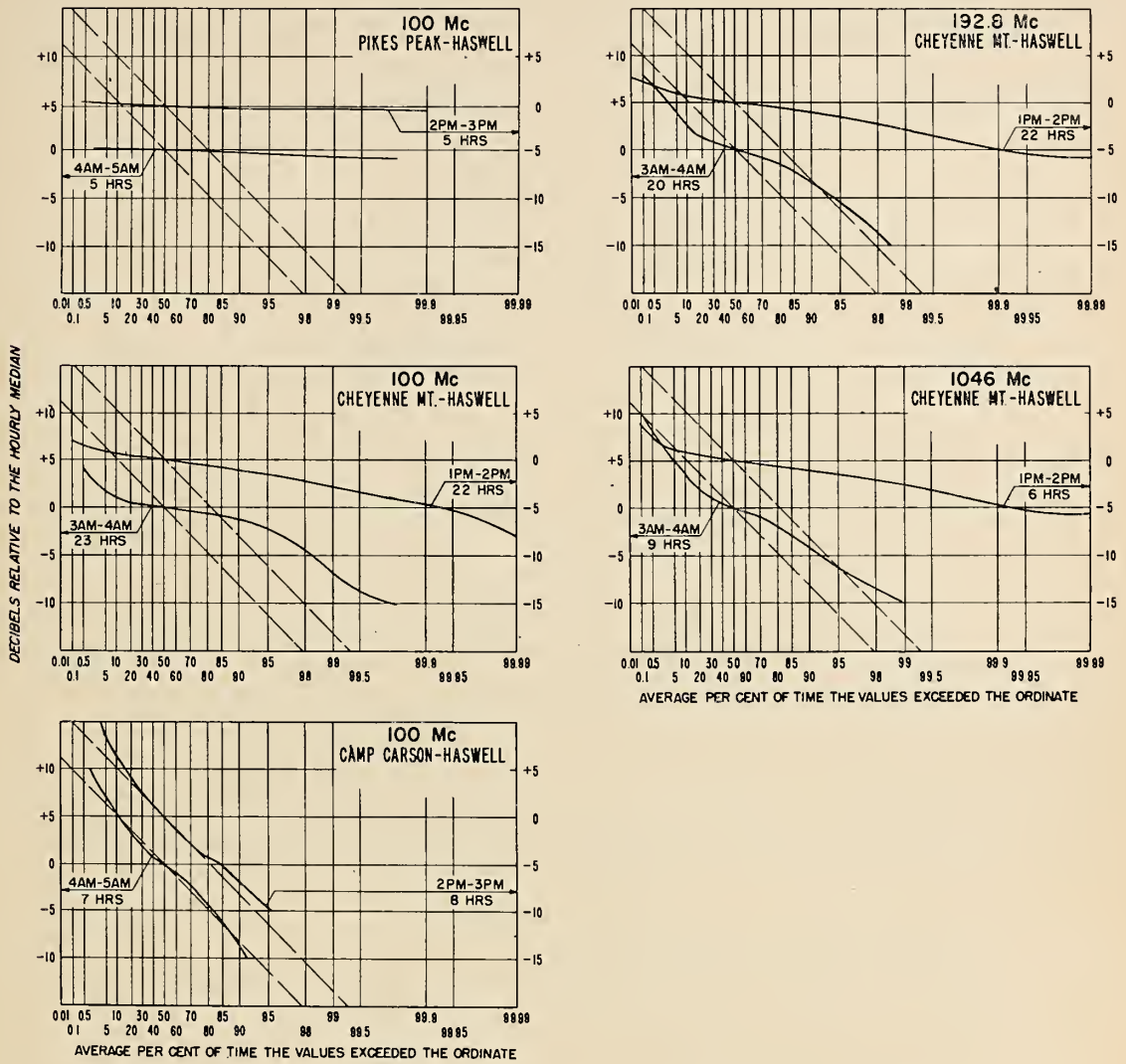


FIGURE 35. Average distributions of instantaneous signal levels, Haswell, August 1952.

Broken line represents Rayleigh distribution.

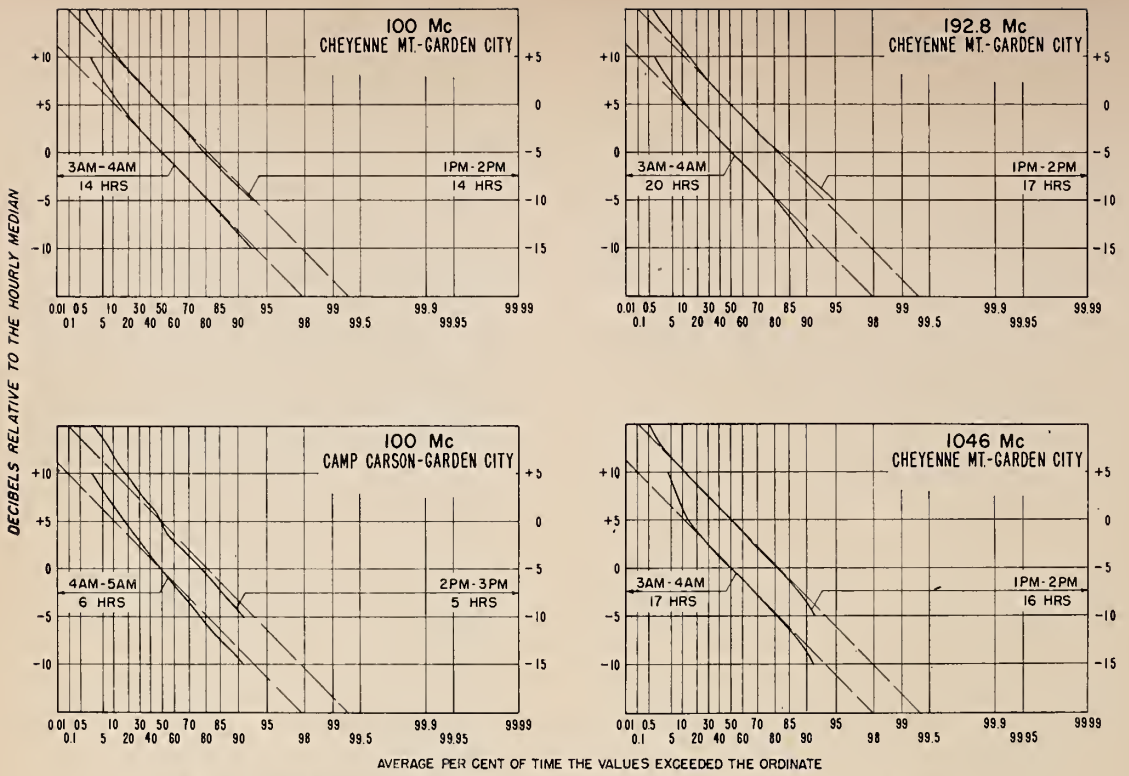


FIGURE 36. Average distributions of instantaneous signal levels, Garden City, August 1952. Broken line represents Rayleigh distribution.

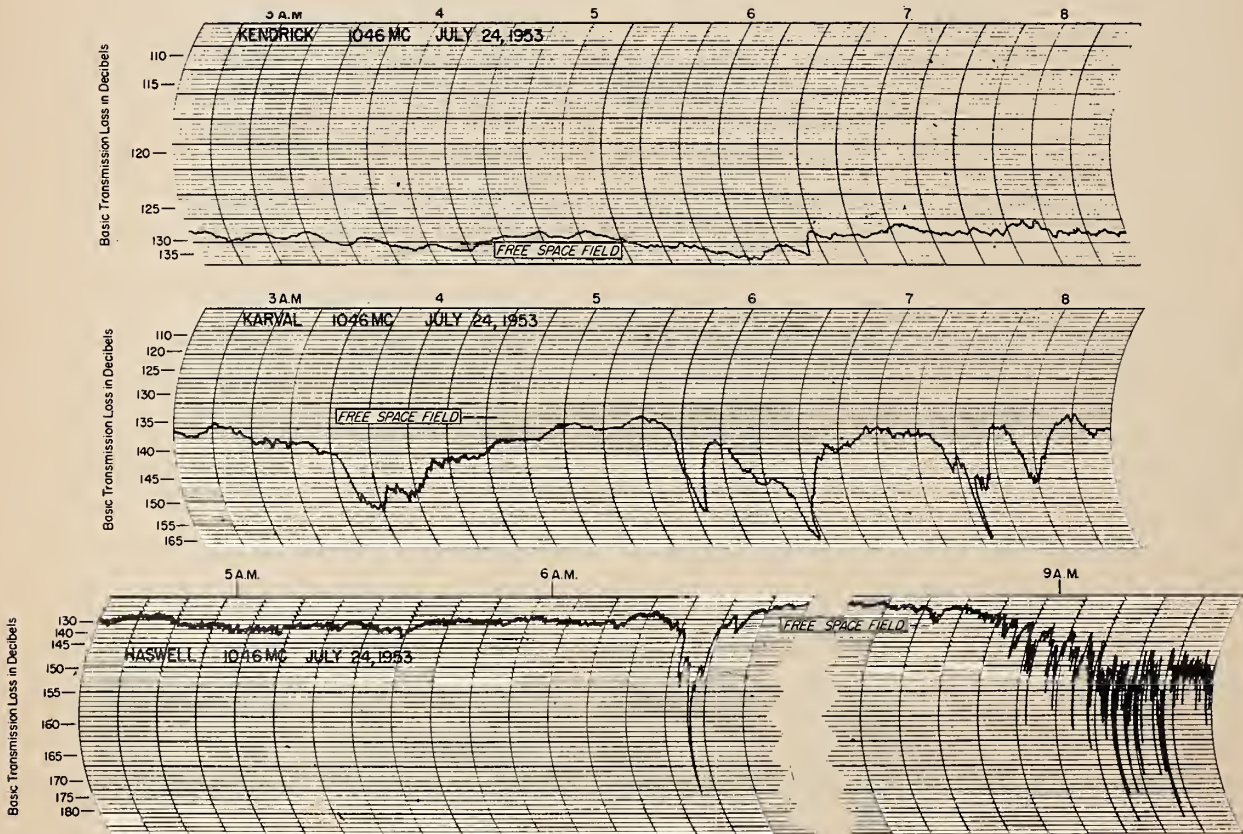


FIGURE 37. Sample of prolonged space-wave fadeouts on 1,046 Mc.

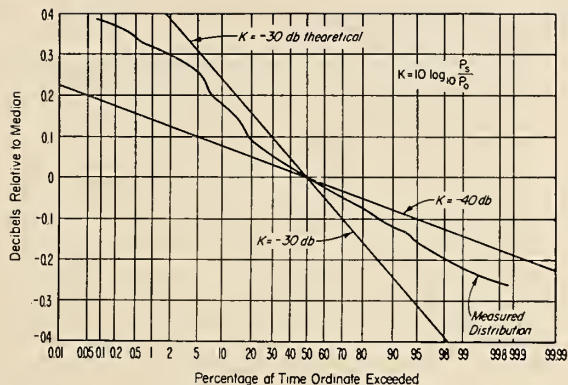
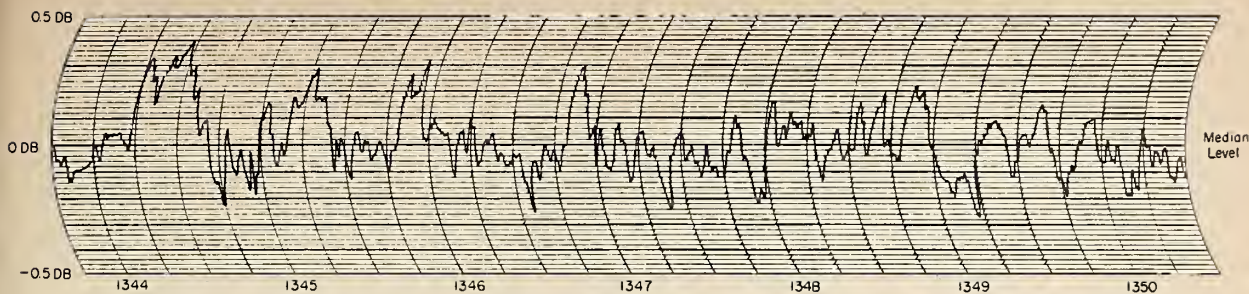


FIGURE 38. *Sample 100-Mc fading record and distribution within radio horizon.*
 Cheyenne Mountain to Kendrick, 49.3 mi; August 6, 1953.

curing at 7 a. m. on April 21, 1953. A more complete study of the fadeouts observed in 1952 is contained in a recent paper by Bean [6].

5.7. Other Studies

Additional measurements and studies include correlation between signals received simultaneously on similar antennas spaced at variable distances in three dimensions and height-gain studies within and beyond the radio horizon. These measurements serve as a basis for a test of the scattering and related theories, as will be described later on.

The employment of the gain-stable receivers described above in conjunction with a differential voltage recorder permits a study of the scattered component of field which is present even well within the radio horizon. Preliminary tests indicate that these variations are small as compared to the median level of the receiver signal but exhibit a substantial fading rate. Figure 38 shows a sample of the output obtained at Kendrick from the differential voltage recorder operating on 100 Mc and illustrates the relative magnitude (less than ± 0.5 db) of the scattered component. The time scale provides an estimate of the fading rate.

Records from measurements made with mobile or semimobile equipment are analyzed in the same way as records from the fixed sites. In every instance the exact methods of handling data are determined by the purpose of the special measure-

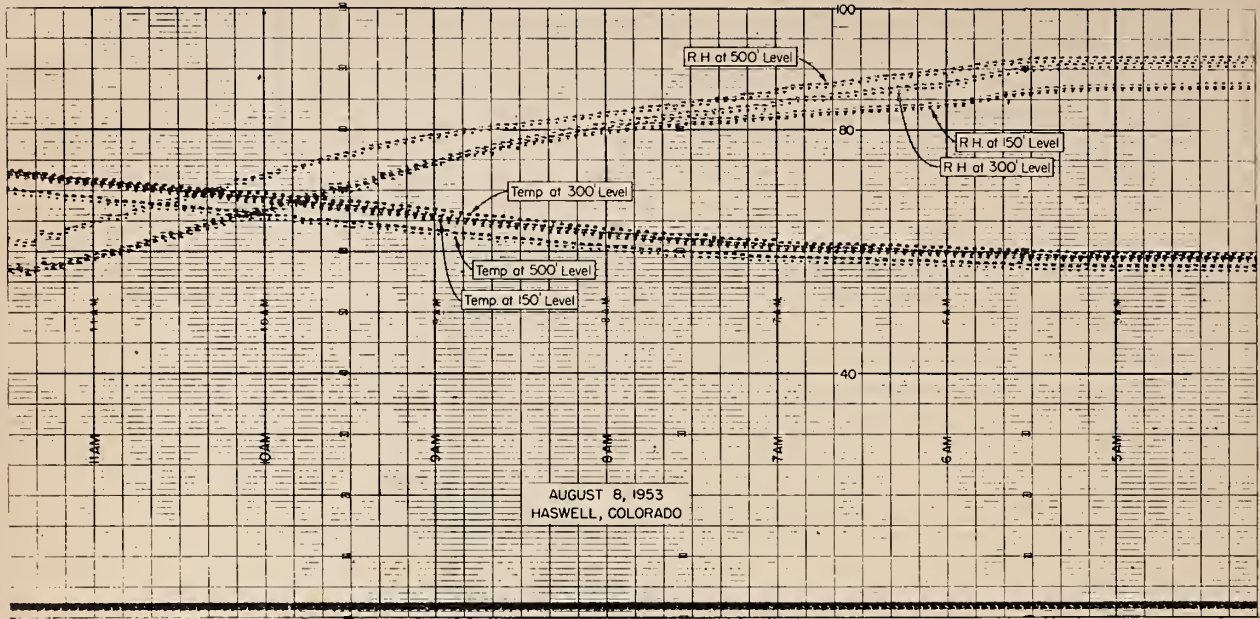
ments and by the amount of data available for each special study.

5.8. Analysis of Meteorological Observations

Records obtained from the instruments mounted on the 500-ft tower at Haswell, and elsewhere, are given a preliminary examination for major phenomena (such as ducting) and are later analyzed in detail statistically. Figure 39 shows a sample record and information derived therefrom. The results of the preliminary evaluation are first examined in the light of pertinent radio propagation records, whereas the results of the more detailed statistical analysis will provide data for the determination of the diurnal and seasonal fluctuations of the refractive index gradient.

A comparison of data from various types of recording instruments will provide means of deciding whether it might be feasible to use some of the more easily obtainable parameters (such as surface wind, pressure, and temperature) as indications of the behavior of the refractive index gradient, or possibly directly as a means of predicting radio propagation conditions.

Short-term measurements with refractometers at various fixed and mobile levels will be analyzed by various methods of auto- and cross-correlation to determine the magnitude of refractive index fluctuations and their spacial distributions, both of which have been found to be important in the scattering of radio frequency energy in the troposphere.



N PROFILES AT HASWELL, COLORADO, AUGUST 8, 1953

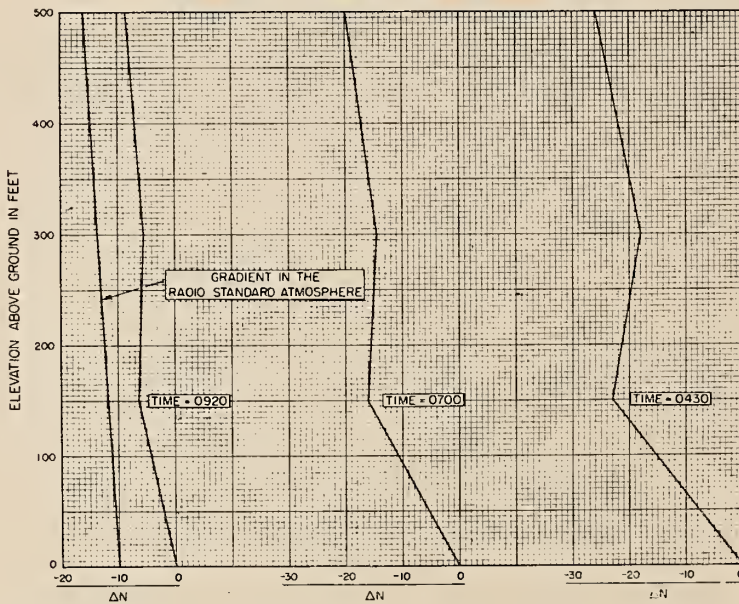


FIGURE 39. Sample of meteorological record and derived N profiles.

6. Preliminary Results in Terms of Theory

6.1. General

The collection of radio propagation and associated meteorological data in the manner described in the preceding sections is only one phase of the complete program. It is also necessary to evaluate results of measurements in relationship to various theories which aim to explain the mechanisms involved in radio wave propagation. This is done not only to test the theories themselves, but also in order to draw conclusions on the general applicability of the results obtained by performing experiments along one single path. If, for instance, a certain observed propagation phenomenon could be uniquely explained by a definite concurrent meteorological condition, it is reasonable to assume that the same meteorological condition, even if occurring in some other part of the country, would produce similar propagation phenomenon. It is also quite important to compare results of measurements constantly with current theories. Modification in the theories may be suggested thereby which, in turn, might influence the design of further experiments. The following paragraphs will deal with several propagation theories as seen in the light of some of the results of the Cheyenne Mountain experiment, although a more complete evaluation will be left to subsequent publications.

6.2. Propagation Within the Radio Horizon

Methods for computing the transmission loss within the radio horizon generally apply to a simplified model consisting of a smooth, spherical earth surrounded by an atmosphere with a refractive index which varies linearly with height. In order to apply these methods to an actual path, such as shown in figure 2, a procedure must be found to replace the actual terrain by a smooth surface. The terrain roughness relative to this smooth surface may then be evaluated in terms of a correction factor applied to the results obtained by the smooth-earth theory. The assumed linear refractive index profile can be taken into account by multiplying the actual radius of the earth by an appropriate factor [7]. This particular method, however, does not apply to propagation effects which arise due to departure from a linear index profile.

A method for replacing the rough terrain by a second-degree smooth surface has been developed by Norton [8]. A suitable criterion of terrain roughness may then be used to study the deviation of measured transmission loss values to the ones computed by application of the smooth-

earth theory. Rayleigh's criterion of roughness has been used in tests of this kind as a measure of the phase incoherence of the energy reflected from the ground as introduced by terrain irregularities. Rayleigh's criterion is usually expressed in the form:

$$R = \frac{4\pi\Delta h \sin \psi}{\lambda},$$

where ψ denotes the grazing angle, λ the wave length of the signal being measured, and Δh the root mean square of the deviations of the actual terrain from the smooth surface used in computing the field. These deviations are taken at equal intervals over the region considered significant in the particular propagation mechanism.

This method has been tested by establishing a series of measuring points well within the radio horizon of the Cheyenne Mountain transmitting sites and comparing measured values of transmission loss at these points to values computed in the manner described above. The deviations of measured from computed values have been plotted against values for Rayleigh's criterion computed for each point as shown in figure 40. It appears from these results that this method of computation of transmission loss will give results in close accord with measurements, provided R is less than say 0.1. It is planned to extend the scope of these measurements to a study of transmission loss versus receiving antenna height for each point, thereby providing a substantially greater amount of data for a test of the applicability of Rayleigh's criterion.

For the locations used in the experiment described above, variations in transmission loss due to changes in the refractive index gradient were assumed to be small, and of the order of the accuracy of the measurements themselves. This assumption is substantiated by a study of the diurnal and month-to-month variations of transmission loss data collected at the fixed receiving site nearest to the Cheyenne Mountain transmitters.

For each of the fixed receiving sites the observed hour-to-hour variations in transmission loss are primarily a function of the change in the refractive properties of the atmosphere. Under the two assumptions of a linear refractive index gradient and replacement of the actual terrain by a smooth surface, the expected transmission loss values at the Karval receiving site have been computed, and are shown in figure 41 plotted versus the effective earth radius factor k . Computations for various types of nonlinear profiles are contemplated.

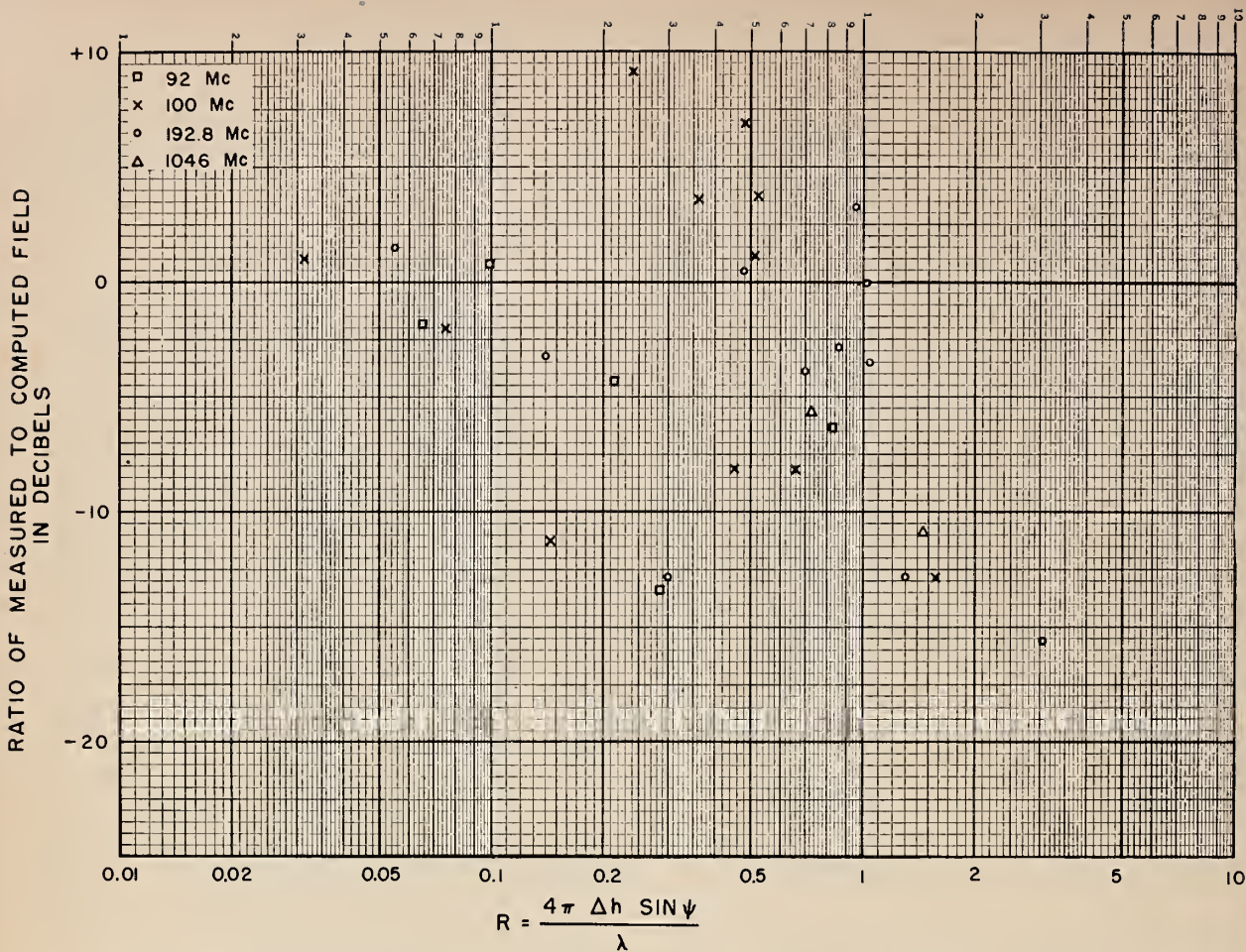


FIGURE 40. Plot of field deviations versus Rayleigh's criterion for Cheyenne Mountain optical paths.

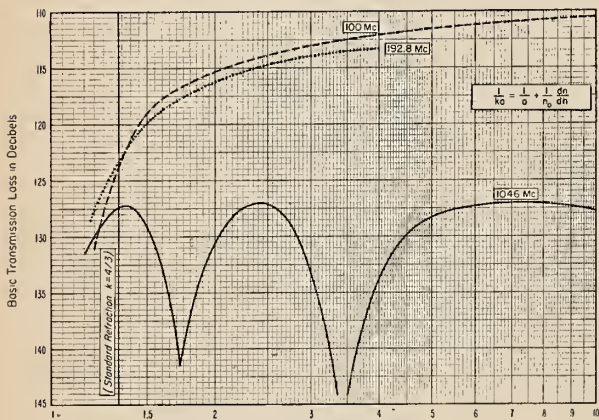


FIGURE 41. Calculated transmission loss for Karval receiving site (within radio horizon) as a function of the refractive index gradient.

Expressed in terms of the effective earth radius factor, k .

6.3. Propagation in the Diffraction Region

Methods to compute transmission loss in the diffraction region beyond the radio horizon are usually based on the assumption of a smooth, spherical earth and a constant gradient of refractive index [9]. The problem, in the case of the Cheyenne Mountain paths, is similar to the one applying to the region within the radio horizon, and consists in finding the best smooth earth replacement for the actual terrain. This includes determination of that portion of the terrain significant in the propagation of radio waves to receiving points beyond the horizon. Studies dealing with this problem are in progress and no final conclusions with regard to methods have been reached. It is also possible with certain types of terrain to consider the radio horizon as a knife edge and compute transmission loss on the basis of knife-edge diffraction [10, 11]. For this purpose criteria have to be developed which would determine the applicability of knife-edge diffraction theory to any particular path.

6.4. Propagation Far Beyond the Radio Horizon

As a result of the availability of a system with a large margin of detectability (due to the use of narrow bandwidths and high transmitter power), it has been possible to investigate the fields received at very great distances. Thus measurable fields have always been available at Anthony, Kans., a distance of 393.5 miles on all frequencies, and at Fayetteville, Ark., a distance of 617.7 miles, they have been found available on 100 Mc at all times and on 1,000 Mc for a few hours. These fields are many orders of magnitude stronger than would be predicted from the diffraction theory of propagation over a smooth earth in a standard atmosphere (e. g., 412 db above that level at Anthony, Kans., on 1,046 Mc) and were tentatively explained in our early work in terms of a theory of partial reflection. As a result of further measurements and theoretical investigation, it is now believed that the Booker-Gordon theory of scattering [12], as elaborated by Staras [13], provides the correct explanation of these intense fields. Some of the analysis leading to this conclusion is given in a recent paper by Herbstreit, Norton, Rice, and Schafer [14].

It is important to emphasize that these scattered signals are of importance not only at large distances beyond the horizon where they constitute the dominant component of the received field but are also important to all shorter distances since they combine with the diffracted field at points near the radio horizon and with the space-wave fields at points within the radio horizon to cause the rapid fading of the received field. A recent paper by Gordon [15] attempts an extension of the scattering theory to points within the radio horizon.

The reduced fading range at the shorter distances (i. e., for negative and small positive values of θ) shown on figure 35 may undoubtedly be explained in terms of the combination of a small scattered Rayleigh-distributed component plus a relatively constant diffracted component. The magnitude of this scattered random component in relation to the steady component of the received field may be estimated by means of the theoretical relation shown in figure 42 in connection with our measured values of the within-the-hour fading range as illustrated in figures 35 and 36. This theoretical relation was derived from results in two papers by Norton [16, 17]. The combination of gain-stable receiver and differential amplifier described in section 3.3.c is being used at the short distances well within the radio line of sight to determine the rapid within-the-hour variations of signal strengths which are very small in comparison to the strong, steady space-wave signal received in this region. Preliminary results of an analysis of a short period of record taken using this technique are shown in figure 38.

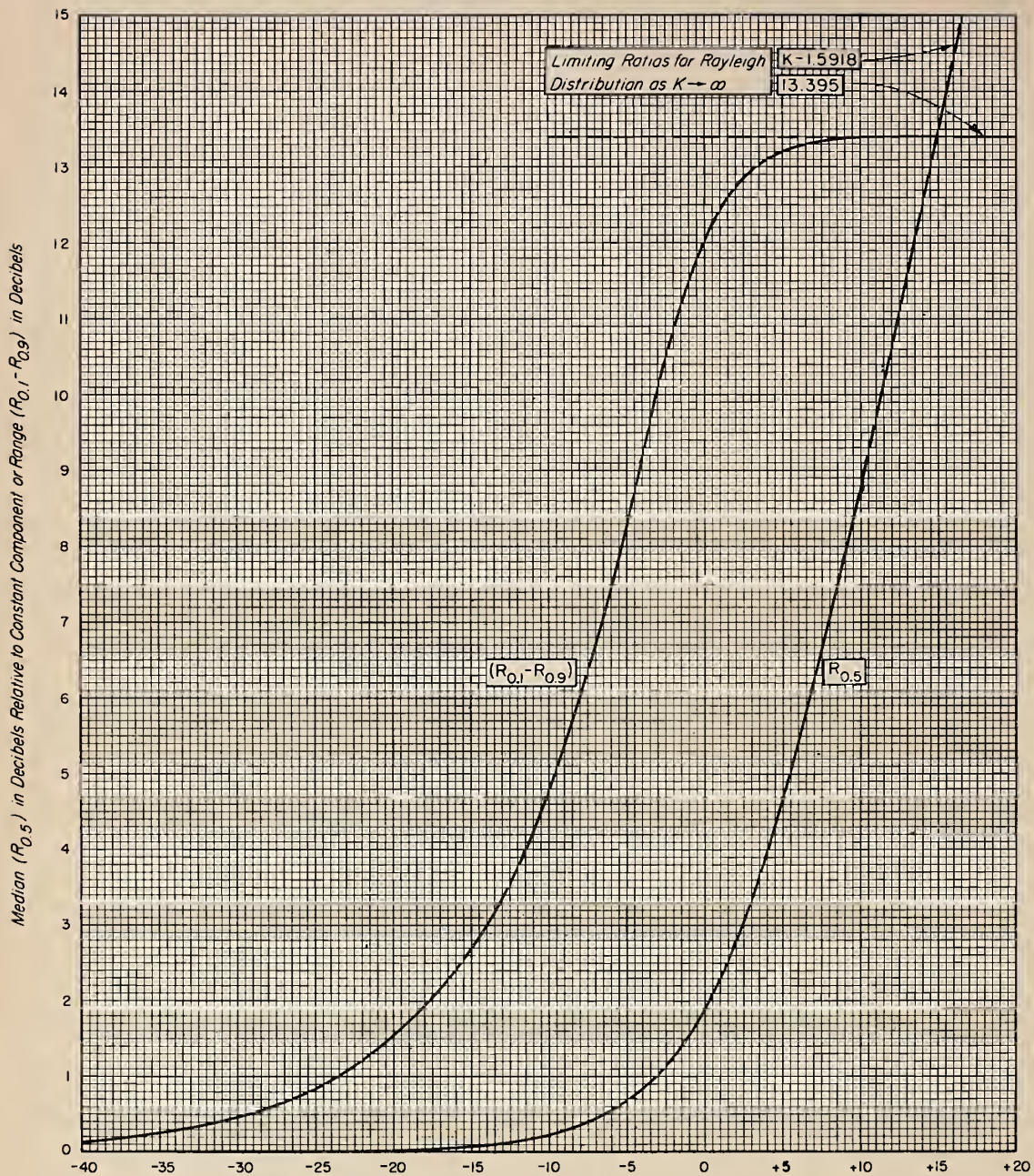
In addition to a knowledge of the magnitudes of the scattered and steady components, we need to know the amount of signal distortion which is likely to arise from the resulting fading. The progress so far made on this latter problem will be described below. Although much further work is required we now have estimated values for the parameters involved and are in a position to make useful engineering estimates of the restriction in effective intelligence-bearing bandwidths resulting from the presence of this scattered component.

Figure 43 shows the results of measurements of the correlation of Cheyenne Mountain transmission as received on spaced antennas at Garden City, Kans. The measurements on 1,046 Mc were fairly complete, being made not only normal to the great circle plane but also vertically and along the path in the great circle plane.

The significance of these measurements in terms of antenna design is more or less obvious, at least in a qualitative way. In order to realize full gain from a receiving antenna, it is necessary that the phase of the received signals be coherent over its entire aperture. Thus, since the correlation is greater for a given separation along the path than normal to the path, the apertures of broadside arrays will be limited to only a few square wavelengths whereas the Yagi or rhombic types of array may be many wavelengths long without a substantial loss in effective gain.

An increase in antenna aperture will, in any case, always result in some increase in gain since more power will be absorbed, but this gain will be less than that expected in free space for large aperture arrays because of the incoherence of the received fields over the large apertures. This same conclusion was reached in the paper on scattering [14] referred to above, and a method was given there for calculating the loss in gain to be expected for a given size of antenna array. Using that method of calculation, the expected total loss in antenna gain has been determined and is shown as a function of the free space gains of the transmitting and receiving antennas and the angular distance, θ , in figure 44.

Before discussing the correlation measurements further it will be instructive to consider the question of antenna height-gain in the scattering region. Figure 45 gives some measurements of height-gain, together with the theoretical curves obtained by the method outlined in the paper on scattering [14]. A portion of this height-gain may be explained simply by noting that the higher receiving antennas can "see" a larger portion of the lower atmosphere, where the scattering parameter $[C(O)/l]$ has a larger value; however, some of the height-gain may be explained by the usual mechanism for explaining height-gain when dealing with completely coherent waves, i. e., that the fields received after ground reflection are nearly



K-Ratio in Decibels of Random Rayleigh Distributed Power to Power in Constant Component

FIGURE 42. Median ($R_{0.5}$) and range ($R_{0.1}$ to $R_{0.9}$) from the cumulative distribution of the resultant amplitude of a constant vector plus a Rayleigh distributed vector.

Power in random component is $(K - R_{0.5})$ db relative to the median level of the cumulative distribution.

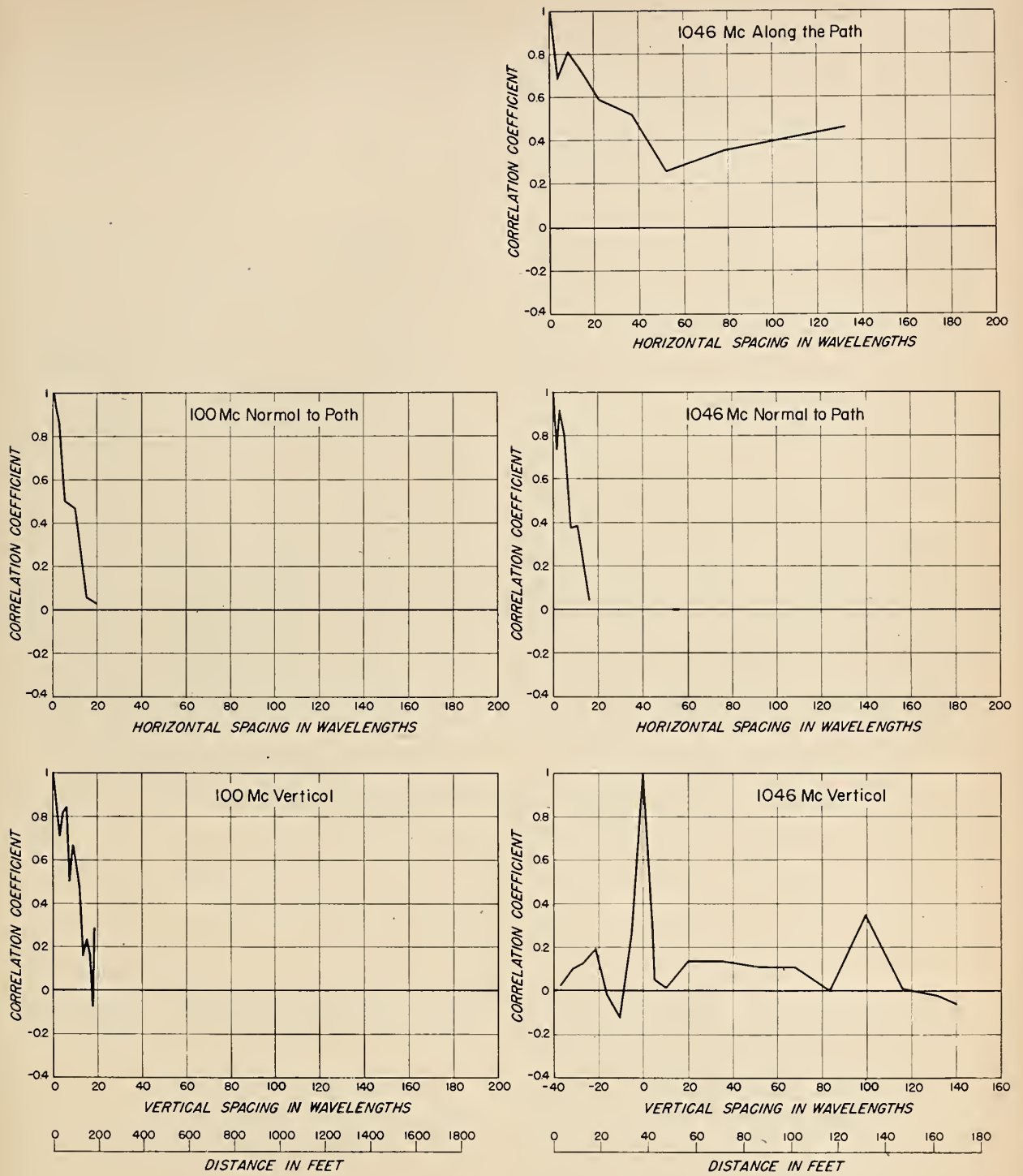


FIGURE 43. Correlation of Cheyenne Mountain field strengths received on spaced antennas at Garden City.

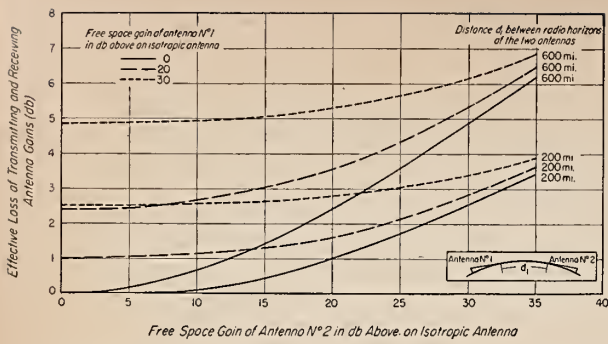


FIGURE 44. Tentative estimate of loss of antenna gain relative to the free space gain.

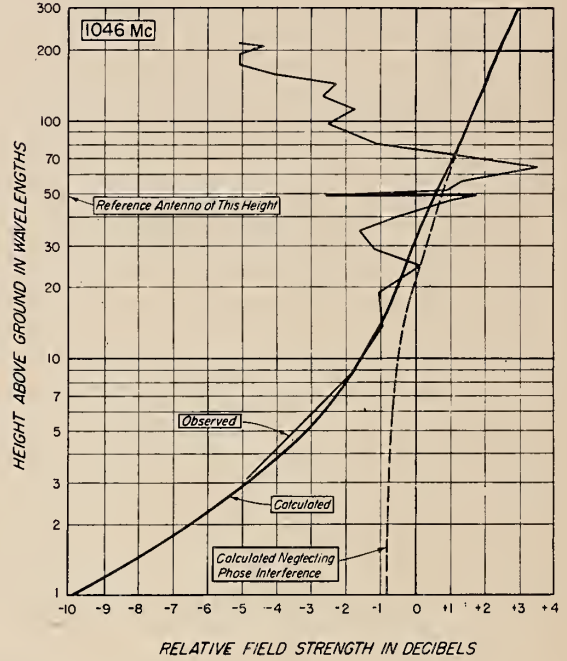
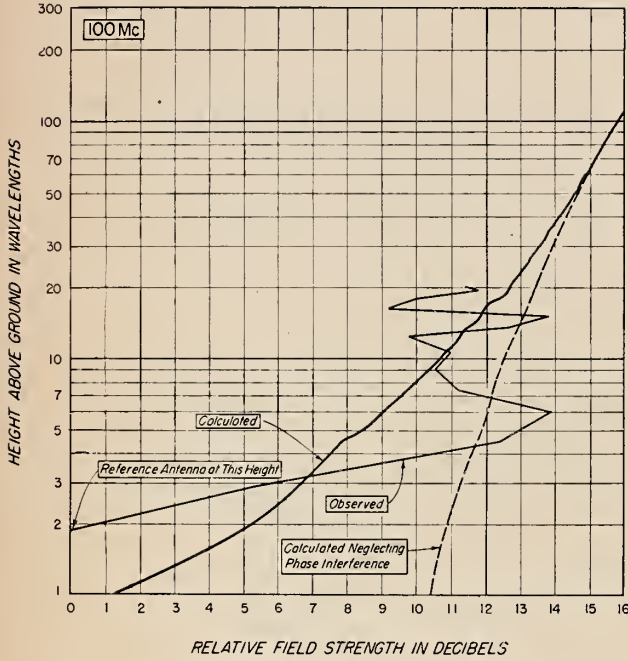


FIGURE 45. Height gain observations at Garden City.

Ratios of median fields observed during 1- to 10-min. periods on vertically spaced antennas.

out of phase with the fields received directly from the scattering medium. The following approximate theoretical discussion of this latter height-gain effect will help in understanding the mechanism involved and will indicate as well the role that correlation plays in the phenomenon.

Let E_a and E_r represent the instantaneous magnitudes of the incident and ground-reflected components of the fields received from the scattering medium. The first approximation will be the assumption that the scattered field may be assumed to arrive at the receiving location from the single elevation angle, ψ_r'' , corresponding to the center of gravity of the scattering medium.

The resultant field at the receiving antenna may then be approximated by the expression

$$\begin{aligned}
 E &= E_a \exp \left[-j2\pi \frac{h_r}{\lambda} \sin \psi_r'' \right] \\
 &\quad - E_r \exp \left[+j2\pi \frac{h_r}{\lambda} \sin \psi_r'' \right] \\
 &= (E_a - E_r) \cos \left[2\pi \frac{h_r}{\lambda} \sin \psi_r'' \right] \\
 &\quad - j(E_a + E_r) \sin \left[2\pi \frac{h_r}{\lambda} \sin \psi_r'' \right],
 \end{aligned}$$

where h_r/λ is the height of the receiving antenna in wavelengths. The negative sign associated with E_r arises from the 180° phase reversal characteristic of waves received near grazing incidence after reflection from the ground. The instantaneous received power is thus proportional to:

$$P \sim E \cdot E^* = (E_d - E_r)^2 \cos^2 \left[2\pi \frac{h_r}{\lambda} \sin \psi_r' \right] \\ + (E_d + E_r)^2 \sin^2 \left[2\pi \frac{h_r}{\lambda} \sin \psi_r' \right].$$

In the above, E^* denotes the conjugate complex value of E . In determining the average power from the above, it should be remembered that the mean value of \bar{E}_r^2 is equal to \bar{E}_d^2 and that the average of $E_d \cdot E_r$ is simply $\rho \bar{E}_d^2$, where ρ is the correlation coefficient between the direct and ground-reflected wave fields.

Thus we obtain for the mean received power:

$$P \sim 2 \bar{E}_d^2 \left[1 - \rho \left\{ \cos^2 \left[2\pi \frac{h_r}{\lambda} \sin \psi_r' \right] \right. \right. \\ \left. \left. - \sin^2 \left[2\pi \frac{h_r}{\lambda} \sin \psi_r' \right] \right\} \right].$$

In order to evaluate the above it is necessary to be able to estimate the value of ρ . An estimate of ρ may be obtained by measuring the correlation of the fields on two antennas, both of which are a large number of wavelengths above the earth, and spaced vertically by an amount $\Delta h = 2h_r$. Thus we may evidently use the results shown in figure 43.

Consider first the case $(\Delta h/\lambda) < 1$ at this distance, where we see by figure 42 that the correlation ρ is approximately equal to unity. In this case the above reduces to

$$\bar{P} \sim 4 \bar{E}_d^2 \sin^2 \left[2\pi \frac{h_r}{\lambda} \sin \psi_r' \right] \quad (\rho = 1),$$

and we see that the received power will increase, since $2\pi(h_r/\lambda)\sin \psi_r'$ is small, as the square of the height in wavelengths.

Next consider the case $[(\Delta h/\lambda) > 10$ at this distance] where the correlation ρ is approximately zero. In this case

$$\bar{P} \sim 2 \bar{E}_d^2$$

and there is no further height gain due to this phase interference phenomenon, the effect of the ground merely doubling the available scattered power at the receiving antenna.

If we set $\Delta h = 2h_r$ in the above, we see that phase interference would be expected to play no further part in the height-gain phenomenon when $(h_r/\lambda) > 5$ at this receiving location. Reference to the meas-

urements shown in figure 45 indicates that this result is roughly substantiated by the data. The height gain above that height increases at a slower rate and is largely due to the fact that the higher antennas "see" lower portions of the atmosphere. Better agreement would scarcely be expected in view of the very approximate nature of the above theoretical derivation. The theoretical height-gain curves compared in figure 45 with the data were derived from the more accurate methods of the paper on scattering [14] and appear to be in fair agreement with the data when consideration is given to the short periods of time involved in these measurements.

One additional qualification to be placed on the experimental height-gain measurements of figure 45 needs to be mentioned. Since the two antennas used for the measurements were mounted on the same vertical mast, they may have interacted to some extent when they were near the same height. This is particularly evident on the 100-Mc data as would be expected since the separation expressed in wavelengths for a given vertical spacing is less at this frequency. This effect probably influenced the 1,046-Mc data to a more limited extent, although there appears to be some evidence of such an effect when (h_r/λ) is near 50.

We turn now to the problem of calculating the correlation coefficient of the fields received on spaced antennas and of the fields received on the same antenna on spaced radio frequencies. The latter problem has a direct relation to the intelligence bearing capacity of the transmission medium. Thus, for example, we would expect distortion of a 5-ke voice communication if the correlation coefficient for frequencies spaced by 5 ke were near zero. Actually, we will find that the transmission medium is expected to be capable of supporting undistorted transmissions over bands of the order of 100 ke in width even at the distance of 226 miles, where the spaced receiver correlation studies were made, and over still wider bands at shorter distances.

We have been able to obtain accurate formal expressions for the correlation coefficient as a function of antenna spacing but have not been able to evaluate the resulting integral expressions in closed form. We are now in the process of evaluating these integrals by numerical methods. In the meantime, although we recognize that the assumed model does not fit the physical situation very well, we have been using the results obtained by Rice [18] for evaluating ρ . Rice assumed that the magnitude of the contributions to the scattered field were normally distributed in all three dimensions with respect to a mean value at the center of gravity. If we let $(Z/\lambda)_\rho$ denote the separation normal to the path at which the correlation coefficient of the fields for antennas spaced by this distance is ρ , then we may use Rice's equations (5) and (9) to determine the frequency separation Δf (in cycles per second) for which the received

fields will have this same correlation coefficient ρ :

$$\Delta f = (Z/\lambda)_\rho C/r \ 2 \sin(\psi_r''/2).$$

In the above, C is the velocity of light in the medium, r the distance and ψ_r'' the angular elevation in radians of the center of gravity of the scattering volume from the receiving location. If we neglect the variation of the scattering parameter $C(O)/l$ with height, it may be shown that $\psi_r'' = \theta$, where θ is defined in figure 6; if the variations of $C(O)/l$ are allowed for, then $\psi_r'' < \theta$. Consequently, if we use θ as an estimate of ψ_r'' , we will underestimate Δf . For the Garden City path $\theta = 0.027$ radian, $r \cong 100$ miles, and we obtain

$$\Delta f > (Z/\lambda)_\rho \frac{186000}{100 \times 0.027} = 69,500 (Z/\lambda)_\rho.$$

If we take $(Z/\lambda)_\rho = 1.5$ corresponding to $\rho \cong 1$, as may be seen on figure 42, we find that $\Delta f > 100$ kc. This effective bandwidth may be expected to increase rapidly with decreasing distance, since $(Z/\lambda)_\rho$ will increase while θ will decrease.

It would be noted that the above is based on

a very approximate theoretical analysis of this problem, and it should be verified by further theoretical and experimental work.

The foregoing presentation indicates the scope of theoretical and experimental knowledge derived from the experiment to date. Final theoretical answers to the many complex problems encountered in evaluating tropospheric propagation data is a field for future research.

The early contributions to the Cheyenne Mountain project by G. R. Chambers and J. H. Chisholm, both of whom have now left the National Bureau of Standards are acknowledged. They were largely responsible for the design, procurement, and installation of the major items of equipment in current use.

The authors express their appreciation to K. A. Norton for his numerous contributions to the theoretical explanation of the results and to the many Cheyenne Mountain staff members who so capably performed their tasks and without whom this paper could not have been written.

7. References

- [1] R. H. Varian, Recent developments in klystrons, *Electronics* [4] **25**, 112 (1952).
- [2] N. Hiestand, High power UHF klystron amplifier design, Convention Record of the IRE 1953 National Convention, pt. 4, p. 129 (March 1953).
- [3] G. E. Boggs, Improvement in gain stability of the superheterodyne mixer through the application of negative feedback, *Proc. IRE* [2] **40**, 202 (1953).
- [4] G. Birnbaum, A recording microwave refractometer, *Rev. Sci. Inst.* [2] **21**, 169 (1950).
- [5] K. A. Norton, Transmission loss in radio propagation, *Proc. IRE* **41**, 146 (1953).
- [6] B. R. Bean, Prolonged space-wave fadeouts at 1,046 Mc observed in Cheyenne Mountain propagation program, *Proc. IRE* **42**, 848 (1954).
- [7] J. C. Schelleng, C. R. Burrows, and E. B. Ferrell, Ultra short wave propagation, *Proc. IRE* **21**, 427 (1933).
- [8] K. A. Norton, Transmission loss of space waves, propagated over irregular terrain, *Trans. IRE Professional Group on Antennas & Propagation*, No. PGAP-3, pp. 152-166 (August 1952).
- [9] K. A. Norton, Calculation of ground wave field intensity over a finitely conducting spherical earth, *Proc. IRE* **29**, 623 (1941).
- [10] K. Bullington, Propagation of UHF and SHF waves beyond the horizon, *Proc. IRE* **38**, 1221 (1950).
- [11] F. H. Dickson, J. J. Egli, J. W. Herbstreit, and G. S. Wickizer, Large reductions of VHF transmission loss and fading by the presence of a mountain obstacle in beyond-line-of-sight paths, *Proc. IRE* **41**, 967 (1953).
- [12] H. G. Booker and W. E. Gordon, A Theory of Radio Scattering in the Troposphere, *Proc. IRE* [4] **38**, 401 (1950).
- [13] Harold Staras, Scattering of electromagnetic energy in a randomly inhomogeneous atmosphere, *J. Appl. Phys.* [10] **23**, 1152 (1952).
- [14] J. W. Herbstreit, K. A. Norton, P. L. Rice, and G. E. Schafer, Radio wave scattering in tropospheric propagation, 1953 Institute of Radio Engineers Convention Record.
- [15] W. E. Gordon, Radio scattering applied to optical links, Report on Symposium on Tropospheric Wave Propagation Within the Horizon, p. 67 (Navy Electronics Laboratory, San Diego, California, March-April 1953).
- [16] K. A. Norton, Propagation in the FM broadcast band, *Advances in Electronics* **1**, 406 (Academic Press, Inc., New York, N. Y., 1948).
- [17] K. A. Norton, Propagation over rough terrain, Report on Symposium on Tropospheric Wave Propagation, pp. 101-105 (U. S. Navy Electronics Laboratory, San Diego, Calif., July 1949).
- [18] S. O. Rice, Statistical fluctuations of radio field strength far beyond the horizon, *Proc. IRE* [2] **41**, 274 (1953).

8. Appendix. Calculation of the Angular Distance, θ Over Irregular Terrain

We see by figure 6 that the angular distance θ , denoted below by $(\alpha_0 + \beta_0)$ is simply equal, over a smooth spherical earth, to the distance between the horizons of the transmitting and receiving antennas divided by the effective radius of the earth, a :²

$$\theta = \frac{d - d_{L_t} - d_{L_r}}{a} \quad (1)$$

Figure 46 shows the geometry involved to take into account the effect of irregular terrain on the determination of α_0 ; a similar geometry is involved in the determination of β_0 .

From this geometry it may be shown that:

$$\alpha_0 = \frac{d}{2a} - \frac{d_{L_t}}{a} + \frac{(h_{ts} - h_{rs})}{d} - \delta_t \quad (2)$$

$$\beta_0 = \frac{d}{2a} - \frac{d_{L_r}}{a} - \frac{(h_{ts} - h_{rs})}{d} - \delta_r \quad (3)$$

where

$$\delta_t = \frac{h_{ts} - h_{L_t} - \frac{d_{L_t}^2}{2a}}{d_{L_t}} \quad (4a)$$

$$\delta_r = \frac{h_{rs} - h_{L_r} - \frac{d_{L_r}^2}{2a}}{d_{L_r}} \quad (4b)$$

$$\theta \equiv \alpha_0 + \beta_0 = \frac{d - d_{L_t} - d_{L_r}}{a} - \delta_t - \delta_r \quad (5)$$

In the above d_{L_t} and d_{L_r} denote the actual distances to the radio horizons as determined from the

² The symbol a is used for simplicity to denote ka' , where a' denotes the actual radius of the earth.

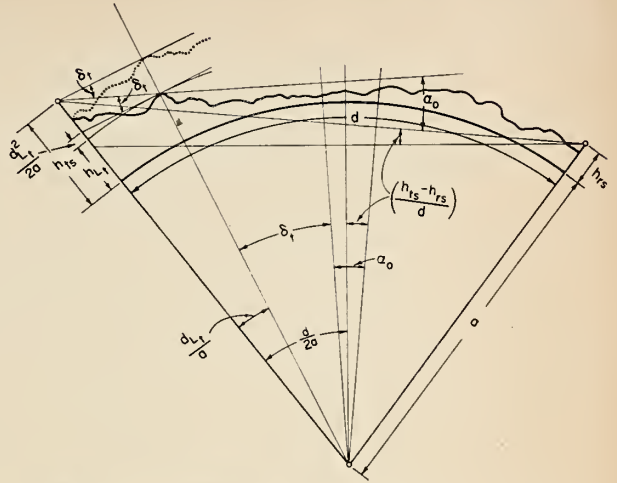


FIGURE 46. Geometry for irregular terrain calculations.

terrain profiles plotted for the path, h_{L_t} and h_{L_r} denote the heights above sea level of the terrain at the respective horizons, and h_{ts} and h_{rs} denote the antenna heights above the same reference, sea level. The distance to the radio horizon, d_{L_t} , is determined by plotting on linear graph paper the heights, $h_T(x)$, above sea level of the actual terrain at the distances, x , corrected for the effects of the normal earth's curvature and of air refraction [$h_T(x) - (x^2/2a)$], versus the distance. The farthest unobstructed point on the terrain, as determined on this modified plot, is the radio horizon, and the distance to this point is denoted by d_{L_t} ; this is the same procedure as that used by Norton [8] in a recent paper.

BOULDER, May 13, 1954.

PERIODICALS OF THE NATIONAL BUREAU OF STANDARDS

The National Bureau of Standards is engaged in fundamental and applied research in physics, chemistry, mathematics, and engineering. Projects are conducted in fifteen fields: electricity and electronics, optics and metrology, heat and power, atomic and radiation physics, chemistry, mechanics, organic and fibrous materials, metallurgy, mineral products, building technology, applied mathematics, data processing systems, cryogenic engineering, radio propagation, and radio standards. The Bureau has custody of the national standards of measurement and conducts research leading to the improvement of scientific and engineering standards and of techniques and methods of measurement. Testing methods and instruments are developed; physical constants and properties of materials are determined; and technical processes are investigated.

Journal of Research

The Journal presents research papers by authorities in the specialized fields of physics, mathematics, chemistry, and engineering. Complete details of the work are presented, including laboratory data, experimental procedures, and theoretical and mathematical analyses. Annual subscription: domestic, \$4.00; foreign, \$5.25.

Technical News Bulletin

Summaries of current research at the National Bureau of Standards are published each month in the Technical News Bulletin. The articles are brief, with emphasis on the results of research, chosen on the basis of their scientific or technologic importance. Lists of all Bureau publications during the preceding month are given, including Research Papers, Handbooks, Applied Mathematics Series, Building Materials and Structures Reports, Miscellaneous Publications, and Circulars. Each issue contains 12 or more two-column pages; illustrated. Annual subscription: domestic, \$1.00; foreign, \$1.35.

Basic Radio Propagation Predictions

The Predictions provide the information necessary for calculating the best frequencies for communication between any two points in the world at any time during the given month. The data are important to all users of long-range radio communications and navigation, including broadcasting, airline, steamship, and wireless services, as well as to investigators of radio propagation and ionosphere. Each issue, covering a period of one month, is released three months in advance and contains 16 large pages, including pertinent charts, drawings, and tables. Annual subscription: domestic, \$1.00; foreign, \$1.25.

Order all publications from the Superintendent of Documents
U. S. Government Printing Office, Washington 25, D. C.

